Clim. Past Discuss., https://doi.org/10.5194/cp-2019-56
Manuscript under review for journal Clim. Past
Discussion started: 24 May 2019

Climate of the Past Discussions

Did the Roman Empire affect European climate? A new look at the effects of land use and anthropogenic aerosol emissions

Anina Gilgen[1], Stiig Wilkenskjeld[2], Jed O. Kaplan[3,4], Thomas Kühn[5,6], and Ulrike Lohmann[1]

[1]ETH Zürich, Institute for Atmospheric and Climate Science, Zurich, Switzerland
[2]Max Planck Institute for Meteorology, Hamburg, Germany
[3]Institute of Geography, University of Augsburg, Augsburg, Germany
[4]Department of Earth Sciences, University of Hong Kong, Hong Kong, China
[5]Atmospheric Research Centre of Eastern Finland, Finnish Meteorological Institute, Kuopio, Finland
[6]Aerosol Physics Research Group, University of Eastern Finland, Kuopio, Finland

Correspondence: Ulrike Lohmann (ulrike.lohmann@env.ethz.ch)

Abstract. As one of the first transcontinental polities that led to widespread anthropogenic modification of the environment, the influence of the Roman Empire on European climate has been studied for more than 20 years. Recent advances in our understanding of past land use and aerosol-climate interactions make it valuable to revisit the way humans may have affected the climate of the Roman Era. Here we drive the global aerosol-enabled climate model ECHAM-HAM-SALSA with land use maps and novel estimates of anthropogenic aerosol emissions from the Roman Empire at its apogee to quantify the effect of humans on regional climate. In a factorial study, we used the HYDE and KK11 anthropogenic land cover change scenarios with three estimates (low, medium, high) of aerosol emissions from fuel combustion and burning of agricultural land.

Land use effects on climate varied from no influence using the HYDE scenario to a significant warming over land of $0.15\,\mathrm{K}$ with KK11 relative to a no-land use control. This warming is primarily caused by regional decreases in turbulent fluxes, in contrast to previous studies that emphasised changes in albedo and evapotranspiration. Aerosol emissions from agricultural burning were greater than those from fuel consumption, but on the same order of magnitude. All emissions scenarios result in an enhanced cooling effect of clouds over a no-emissions control scenario. As a consequence, the land surface temperature averaged over our entire study domain decreased significantly by $0.17\,\mathrm{K}$, $0.23\,\mathrm{K}$, and $0.46\,\mathrm{K}$ for the low, the intermediate, and the high emissions scenarios, respectively. Cooling caused by aerosol emissions is largest over Central and Eastern Europe, while warming caused by land use occurs in parts of North Africa and the Middle East. Our results suggest that the influence of Roman Era anthropogenic aerosol emissions on European climate may have been as important as that of deforestation and other forms of land use. Our model may overestimate aerosol-effective radiative forcing, however, and our results are very sensitive to the inferred seasonal timing of agricultural burning practices and natural aerosol emissions over land (wildfire emissions and biogenic emissions). Nevertheless, it is likely that human influence on land and the atmosphere affected continental-scale climate during Classical Antiquity.

Clim. Past Discuss., https://doi.org/10.5194/cp-2019-56
Manuscript under review for journal Clim. Past
Discussion started: 24 May 2019

Climate of the Past Discussions

1 Introduction

Humans shaped the European landscape thousands of years before the Industrial Revolution (Kaplan et al., 2016) primarily through deforestation, which was applied for several purposes: less dense forests facilitated hunting, foraging, and mobility (Kaplan et al., 2016), removal of trees was required for most forms of agricultural land use (Klein Goldewijk et al., 2011), and wood was harvested for fuel or as timber for manufacturing and building purposes (Harris, 2013). The replacement of forests by other vegetation types influences climate through both biogeochemical and biogeophysical effects (Bathiany et al., 2010). Biogeochemical effects occur primarily through changes in the chemical composition of the atmosphere, e.g. transfers of carbon from land to atmosphere, where it resides as the greenhouse gas CO_2. Because atmospheric CO_2 is long-lived and well mixed, biogeochemical effects have a global impact on climate (Boysen et al., 2014). In contrast, biogeophysical effects rather act at regional scale. These include changes in physical land surface characteristics, such as roughness length or surface albedo (Claussen et al., 2001). Increases in surface albedo due to deforestation usually lead to a cooling, while changes in energy redistribution (evaporative fraction and turbulent flux) are associated with a warming (Lee et al., 2011). The net effect of biogeophysical effects on temperature is a strong function of radiation and thus latitude (Lee et al., 2011; Li et al., 2016c): in the tropics, changes in energy redistribution usually dominate; as a consequence, deforestation induces a net warming. In high latitudes, changes due to surface albedo are generally more important, and deforesation thus leads to a net cooling.

Smith et al. (2016) modelled the impact of biogeophysical effect during the Holocene and found that anthropogenic land cover change in Europe and East Asia had significant impacts on climate (temperature, precipitation, and near surface wind speed) already a few thousand of years ago. They used the reconstruction of anthropogenic land cover change from Kaplan and Krumhardt (KK10; Kaplan et al., 2009, 2011) for their simulations.

Humans also affect the climate by aerosol emissions. Aerosol particles absorb and scatter radiation, which leads to a radiative forcing due to aerosol-radiation interactions ($\mathrm{RF_{ari}}$). Furthermore, aerosols affect clouds by heating atmospheric layers when they absorb a considerable amount of the solar radiation (Koch and Del Genio, 2010). Depending on the cloud type and the position of the aerosol layer relative to the cloud, cloud cover can either decrease or increase (Koch and Del Genio, 2010). Together with $\mathrm{RF_{ari}}$, these absorption-related adjustments are called $\mathrm{ERF_{ari}}$ (effective radiative forcing due to aerosol-radiation interactions).

Aerosols further impact radiation indirectly by influencing the number of cloud droplets as well as ice crystals. Aerosols that activate into cloud droplets are called cloud condensation nuclei (CCN). If the CCN concentration increases at a fixed cloud liquid water content, then the cloud droplet number concentration (CDNC) generally also increases, which enhances the backscattering of radiation (Twomey, 1974, 1977). This effect is called $\mathrm{RF_{aci}}$ (radiative forcing due to aerosol-cloud interactions; Boucher et al., 2013) and generally increases the cooling effect of clouds. An increase in CCN (and thus CDNC) can also have other effects, e.g. affecting the cloud lifetime by decelerating collision-coalescence (Albrecht, 1989). Together with $\mathrm{RF_{aci}}$, such adjustments are called $\mathrm{ERF_{aci}}$ (effective radiative forcing due to aerosol-cloud interactions; Boucher et al., 2013).

Clim. Past Discuss., https://doi.org/10.5194/cp-2019-56
Manuscript under review for journal Clim. Past
Discussion started: 24 May 2019

Climate of the Past Discussions

It is not straightforward to disentangle all these different aerosol effects. Here, we define the aerosol radiative effect (ARE) and the cloud radiative effect (CRE) as the differences between radiative fluxes at the top of the atmosphere in the presence and absence of aerosols and clouds, respectively. These quantities can be calculated with a climate model by a double call of the radiation scheme once with and once without aerosols or clouds.

Present-day anthropogenic aerosol emissions are very high compared to pre-industrial emissions. However, when the effect of anthropogenic aerosol emissions on the radiative balance is quantified, it makes a difference whether AD 1850 or AD 1750 is chosen as the reference year (Carslaw et al., 2017). This shows that anthropogenic aerosol emissions probably had an impact on climate already in AD 1850. But when did anthropogenic aerosol emissions start to change the climate? Is it possible that locally significant changes occurred already thousands of years ago?

In the first century AD, the Roman Empire was at its apogee, with a "surprisingly high standard of living" for Antiquity (Temin, 2006). Around the same time, the Han dynasty in China also controlled a large part of the world's population. These two empires had comparable spatial extents and population sizes (Bielenstein, 1986; Scheidel, 2009). Although the global population was approximately 2.6 and 5.5 times smaller in AD 1 than in AD 1700 and AD 1850, respectively (Klein Goldewijk et al., 2017), industrial activites between 100 BC and AD 200 in both Europe and East Asia already left imprints in ice cores and sedimentary records, for example heavy metals and ^{13}C-enriched methane (Hong et al., 1996; Brännvall et al., 1999; Sapart et al., 2012). In cities and towns during Antiquity, smoke emissions were sufficiently severe to darken buildings and to enforce laws against air pollution (Makra, 2015).

Of course, these activities are by no means comparable to the anthropogenic impact on climate under present-day conditions. Nevertheless, we hypothesise that these anthropogenic activities could already have had an influence on climate on a continental scale. The goal of this study is thus to estimate the influence of anthropogenic land cover change and aerosol emissions on climate around AD 100 with a focus on the Roman Empire. We use the global aerosol-climate model ECHAM-HAM-SALSA for this assessment.

To estimate the influence of land use on climate, we compare a control simulation without land use to simulations including crop and pasture areas representative for AD 100. Two different reconstructions of anthropogenic land cover were used. Since ECHAM-HAM-SALSA does not calculate a full carbon cycle, we only investigate biogeophysical effects and not the biogeochemical effects. The impact of anthropogenic land cover on secondary organic aerosol (SOA) precursors is simulated.

To assess the impact of anthropogenic aerosol emissions on climate, we conducted simulations with and without anthropogenic aerosol emissions. We consider anthropogenic emissions from fuel consumption, crop residue burning, and pasture burning. Since crop residue and pasture burning are explictly considered in these sensitivity simulations, the natural fire emissions, which were calculated assuming no anthropogenic land cover, were reduced in order to not overestimate the total fire emissions.

Clim. Past Discuss., https://doi.org/10.5194/cp-2019-56
Manuscript under review for journal Clim. Past
Discussion started: 24 May 2019

2 Methods

We conducted several simulations (Sect. 2.8) with an aerosol-climate model (Sect. 2.1). The simulations aim to represent the Roman Empire at its maximum extent around AD 100 (Fig. S1). Our study domain is a box between $10°$ W and $50°$ E, $20°$ N and $60°$ N, which fully encompasses the Roman Empire at that time. We acknowledge that this definition includes some regions that were not part of the Roman Empire, such as the highly populated Northern Germany, but drawing precise boundaries was challenging due to the coarse spatial resolution of our model, and many of the land use and industrial activities present within the political boundaries of the Roman Empire at this time also occurred outside of it. Since the main focus of our study lies on the anthropogenic influence on climate, and humans near but outside the Roman Empire also carried out agriculture and emitted aerosols, our main conclusions should not be affected by the exact geographical definition. Similarly, some boundary conditions (vegetation, fire emissions) refer to a somewhat earlier period than AD 100 (e.g. AD 1) due to data availability, but concerning the large temporal uncertainties when going so far back in time, we do not consider this to be an issue.

Associated with these experiments, we needed data for i) the boundary conditions (Sect. 2.2), ii) anthropogenic land cover change (Sect. 2.3), and iii) aerosol emissions (Sects. 2.4, 2.5).

2.1 Model

To study potential anthropogenic effects of land cover and aerosols, we used the global aerosol-climate model ECHAM6.3-HAM2.3-SALSA2.0. SALSA stands for Sectional Aerosol module for Large Scale Applications (Kokkola et al., 2008; Bergman et al., 2012; Kokkola et al., 2018). The aerosol size distribution is described with 10 size sections. The aerosol species black carbon (BC), organic matter ($\mathrm{OM} = 1.4 \cdot \mathrm{OC}$, where OC stands for organic carbon), sulfate (SO_4), dust, and sea salt are considered. Particles below $r = 25\,\mathrm{nm}$ comprise exclusively of OM and/or SO_4, whereas larger particles can contain any aerosol species.

The land component of ECHAM-HAM-SALSA is called JSBACH (Jena Scheme for Biosphere–Atmosphere Coupling in Hamburg; Raddatz et al., 2007). In our simulations, heterogeneity in each grid box is represented by geographically varying fractions of 12 different plant functional types. The implementation of anthropogenic land cover change in JSBACH is described in Reick et al. (2013).

2.2 Boundary conditions

The greenhouse gas concentrations follow Meinshausen et al. (2017). Both the greenhouse gas concentrations and the orbital parameters were averaged over AD 50-150 (Table S1). To prescribe natural vegetation fractions (Sect. 2.3), sea-surface temperatures (SST), and sea ice concentrations (SIC) we used output from a simulation with the Earth System Model MPI-ESM (Bader et al., 2019, in review, Fig. S2), called MPI_no_LCC in the following. The annual cycle of SST and SIC was derived by averaging the MPI_no_LCC output from AD 50 to 150. The MPI-ESM model has the same atmospheric core (ECHAM) and uses the same vegetation model (JSBACH) as ECHAM-HAM-SALSA. MPI_no_LCC ran from 6000 BC to AD 1850 and

Clim. Past Discuss., https://doi.org/10.5194/cp-2019-56
Manuscript under review for journal Clim. Past
Discussion started: 24 May 2019

considered slow forcings, i.e. changes in greenhouse gases (CO_2, CH_4, N_2O) and orbital parameters, but no anthropogenic land cover change. Vegetation was calculated dynamically (Brovkin et al., 2009).

For the simulated sulfur cycle and SOA calculation, climatologies for the following oxidants are needed: H_2O_2 (only for sulfur), O_3, OH, and NO_3. In general, it is uncertain how these oxidants have changed over the past millennia. OH concentrations seem to be relatively stable (Pinto and Khalil, 1991; Lelieveld et al., 2002; Murray et al., 2014). In contrast, ice core measurements suggest that H_2O_2 has increased by $> 50\%$ over the last 200 years (Sigg and Neftel, 1991; Anklin and Bales, 1997). Modelling studies suggest that also NO_3 and O_3 have increased since the pre-industrial (Khan et al., 2015; Murray et al., 2014). For O_3, Pinto and Khalil (1991); Crutzen and Brühl (1993) found that the changes are relatively small between the glacial and pre-industrial; however, the ozone profile shows larger changes between pre-industrial and present-day conditions (Crutzen and Brühl, 1993). In line with this, we expect that differences in oxidant concentrations are larger between AD 1850 and present-day than between AD 100 and AD 1850 due to large anthropogenic emissions of various gases since AD 1850. Therefore, we used climatological monthly mean mixing ratios of oxidants representative for AD 1850 conditions (Fig. S2). They were derived from simulations with the Community Earth System Model version 2.0 (CESM2.0) Whole Atmosphere Community Climate Model (WACCM[1]).

2.3 Vegetation and land cover change

In our simulations with ECHAM-HAM-SALSA, natural vegetation was not dynamic. The coverages of different natural vegetation types representative for AD 100 were taken from MPI_no_LCC (Fig. S2). These natural vegetation fractions are fixed over time. They are from an earlier year than AD 100 (end of year 10 BC) because vegetation around AD 1 was used to calculate the fire emissions (Sect. S3).

For the sensitivity simulations in ECHAM-HAM-SALSA, we used two different reconstructions to estimate anthropogenic land cover fractions around AD 100: the anthropogenic land cover reconstructions from KK11 (an update of KK10; Kaplan et al., 2011, 2012), and the reconstructions from the HYDE database version 3.1 (Klein Goldewijk et al., 2011, HYDE11 in the following). The empirical model of KK11 assumes that per capita land use declines over time. In contrast, the reconstruction of cropland and pasture from HYDE11 assumes a nearly constant per capita land use hindcasting approach with allocation algorithms that change over time (Klein Goldewijk et al., 2017). As a consequence, the anthropogenic land cover fraction in the past is considerably higher in the estimate by KK11 compared to the estimate of HYDE11.

KK11 provides information about the fraction of a gridbox subject to anthropogenic land use. For our simulations, we interpolated the values for AD 1 from a $0.5° \times 0.5°$ grid to the Gaussian grid of ECHAM-HAM-SALSA and assumed that the same fraction of natural vegetation is converted to crop and pasture in equal shares. This seems to be a good first order approximation: in the reconstruction of HYDE11, which estimated pasture and crop areas separately, they contribute each roughly 50%, both when averaged over the whole world and when averaged over the study domain. However, there are of course regions (both in HYDE11 and in reality) where either crop or pasture dominated.

[1] https://svn-ccsm-inputdata.cgd.ucar.edu/trunk/inputdata/atm/cam/tracer_cnst/tracer_cnst_WACCM6_halons_3DmonthlyL70_1850climo295_c180426.nc, downloaded: 27 July 2018

Clim. Past Discuss., https://doi.org/10.5194/cp-2019-56
Manuscript under review for journal Clim. Past
Discussion started: 24 May 2019

HYDE11 provides information about the area of crop and pasture (km^2 per gridcell) on a 5' grid. We divided these areas by the maximum land area available per gridcell (also from HYDE11) to get fractions of crop and pasture per land area and interpolated the values to the Gaussian grid of ECHAM-HAM-SALSA.

The anthropogenic land cover fractions were scaled to the fraction of the vegetable part of the model grid. Due to inconsistencies between the data sets and the model setup, including differences in the land sea mask, the actually applied land use changes are smaller than prescribed in the original data sets. In our model, the total crop areas in the study domain amount to $5.46 \cdot 10^5\,\mathrm{km}^2$ and $13.8 \cdot 10^5\,\mathrm{km}^2$ for HYDE11 and KK11, respectively (i.e. 41% and 21% lower than the original estimate). For pasture, the total areas add up to $4.75 \cdot 10^5\,\mathrm{km}^2$ and $13.8 \cdot 10^5\,\mathrm{km}^2$, respectively (41% and 12% lower than the original estimate). For comparison, the total land area in the study domain is $163 \cdot 10^5\,\mathrm{km}^2$ in our model.

2.4 Natural aerosol emissions

Sea salt, dust, and oceanic dimethylsulfide (DMS) emissions are calculated online as described in Tegen et al. (2019). Tropospheric SO_2 emissions from volcanoes are based on Andres and Kasgnoc (1998); Halmer et al. (2002) as described in Stier et al. (2005). To estimate SOA formation from biogenic sources, a volatility basis set (e.g. Donahue et al., 2006) was used, with a simplified one-step oxidation chemistry (Sect. 2.2) to convert SOA precursors into SOA forming species (Kühn et al., 2019, in preparation). The emission strengths of these SOA precursors were calculated online based on the vegetation in the model (Henrot et al., 2017). As a consequence, all ECHAM-HAM-SALSA simulations that include anthropogenic land use account for the effect of these land cover changes on SOA precursor emissions (Table S2). DMS emissions from terrestrial sources were set to present-day values (Pham et al., 1995); the emissions are very low compared to oceanic DMS emissions, though.

Fires have played an important role in shaping the composition and structure of Mediterranean vegetation communities (Naveh, 1975). To simulate past natural fire emissions, we used a stand-alone version of the carbon and vegetation dynamics sub-model of JSBACH (CBALONE; called CBALANCE in Wilkenskjeld et al., 2014) together with the fire submodel SPITFIRE (Thonicke et al., 2010; Lasslop et al., 2014; Rabin et al., 2017). More information can be found in the Supplement (Sect. S3).

2.5 Aerosol emissions from fuel consumption

Many variables influencing the anthropogenic aerosol emissions are highly uncertain. Therefore, three sets of variables respectively leading to low, intermediate and high aerosol emissions were estimated for the Roman Empire based on literature. Figure S8 illustrates how much these scenarios differ.

Anthropogenic emissions associated with both fuel consumption and agricultural burning were likely to have had pronounced regional variations. Despite this variability, we tried to estimate values representative for the whole of our study domain for variables such as fuel consumption or fuel load.

We treated the anthropogenic emissions in the same way as natural fire emissions, except for the emission height. In contrast to the natural fire emissions, for which the simulated emission profile depends on the planetary boundary layer (Veira et al., 2015), we emitted the anthropogenic aerosols at the surface.

Clim. Past Discuss., https://doi.org/10.5194/cp-2019-56
Manuscript under review for journal Clim. Past
Discussion started: 24 May 2019

Climate of the Past Discussions

For fuel consumption, the aerosol emissions EM of species i [$\mathrm{kg_{aerosol}\ m^{-2}\ s^{-1}}$] were estimated using the following equation:

$$EM_i = cons \cdot popd \cdot EF_i, \tag{1}$$

where $cons$ [$\mathrm{kg_{dry\ fuel}\ capita^{-1}\ s^{-1}}$] is the fuel consumption per capita, $popd$ [$\mathrm{capita\ m^{-2}}$] is the population density, and EF is the aerosol emission factor of species i [$\mathrm{kg_{aerosol}\ kg^{-1}_{dry\ fuel}}$]. In the following, we derive estimates for these three variables for the different emission scenarios. We assume that the three variables are independent when calculating the emissions.

2.5.1 Fuel consumption per capita

In the Roman Empire, people produced aerosol particles by burning several types of fuel for different purposes such as cooking, residential heating, heating bath houses, iron production, glass making, pottery production, or cremation (Malanima, 2013; Veal, 2017; Mietz, 2016; Janssen et al., 2017). For iron production, high temperatures are needed, which were only achieved by burning charcoal (Janssen et al., 2017). For other purposes, also wood or agricultural waste products (e.g. olive pits or dung) were used (Mietz, 2016). The Roman Empire consisted of different regions (e.g. rural versus urban; wetter versus drier climate) with different fuel consumptions per capita and different fuel strategies. Presently, it is therefore not possible to estimate the fuel consumption with large confidence.

Malanima (2013) estimates that 1-2 kg of wood were consumed per capita per day in the ancient Mediterranean region. His numbers refer to fuel for residential heating and cooking, while he states that industrial contributions were negligible. In present-day developing countries that mainly depend on fuel wood for producing energy (sometimes used as surrogates for past conditions), typical estimates of domestic fuelwood consumption also range from 1 to 2 kg per capita per day according to Wood and Baldwin (1985). Also the values in Yevich and Logan (2003) are in the same range: for Africa (year 1985), the mean and median of fuelwood consumption over the countries considered are approximately $1.5\,\mathrm{kg}$ per capita per day (assuming 15% moisture content).

Based on the quantitative model from Pompeii, Veal (2017) applied two extreme scenarios for Rome, where the low and the high estimates for fuel consumption are 1 and 2 t per capita per year. This corresponds to 2.7 and $5.4\,\mathrm{kg}$ per capita per day, respectively, which is 2.7 times larger than the estimates by Malanima (2013). The fuel estimates by Veal (2017) however refer to fuel (i.e. the sum of wood and charcoal) in contrast to the estimates by Malanima (2013), which refer to wood (either burnt directly or used for charcoal making; he assumes little contribution from the latter). This distinction is important when calculating emissions because several kilogrammes of wood are needed to make one kilogramme of charcoal, making the difference between the two estimates even larger. While Veal's model derived for Pompeji might give reasonable results for Rome, it is likely not applicable to all parts of the Roman Empire, e.g. in the countryside. Nevertheless, it shows that the fuel consumption in the Roman Empire might have been substantially larger than suggested by Malanima (2013), since the estimates of Veal (2017) account for all types of fuel consumption, including e.g. baths and industrial activites. Recently, Janssen et al. (2017) calculated the wood consumption for the city Sagalassos (2500-3500 inhabitants) to range between 0.6 and $0.8\,\mathrm{kg}$ per capita per day for local pottery production and 1.3-$3.4\,\mathrm{kg}$ per capita per day for heating the bath (oven dry wood). Although

Clim. Past Discuss., https://doi.org/10.5194/cp-2019-56
Manuscript under review for journal Clim. Past
Discussion started: 24 May 2019

Climate of the Past Discussions

Table 1. The values used to calculate the aerosol emissions from fuel consumption (Equation 1) for the low, the intermediate, and the high scenarios. The total population in the study domain is shown instead of the population density (*popd*, used in the equation) since this is more intuitive.

Var.	Unit	Low estimate	Intermediate estimate	High estimate
$cons$	$\mathrm{kg_{dry\ fuel}\ capita^{-1}\ day^{-1}}$	1.5	3	5
Population	10^6	55[a]	82	137
EF_{combined}, BC	$\mathrm{g\ kg^{-1}_{dry\ fuel}}$	0.23	0.37	0.59
EF_{combined}, OC	$\mathrm{g\ kg^{-1}_{dry\ fuel}}$	1.88	2.89	4.45
EF_{combined}, SO_2	$\mathrm{g\ kg^{-1}_{dry\ fuel}}$	0.041	0.10	0.18

[a]Klein Goldewijk et al. (2011)

Sagalassos might differ from other places, this indicates that the neglect of non-residential sources by Malanima (2013) might not be justified, at least in some regions. Based on these different studies, we use 1.5, 3, and 5 kg of fuel (expressed as wood, wood used for charcoal making, or agricultural waste on a dry fuel mass basis) per capita per day for the low, the intermediate, and the high emission scenarios, respectively (Table 1).

In general, more fuel for heating was consumed where and when it was cold (Malanima, 2006; Warde, 2006). However, we do not differentiate between heating, cooking, iron production, and other burning activities in our calculation. Therefore, we assume a constant fuel consumption over the year and over latitudes. As a consequence, the values in summer and in the South might be overestimated, whereas the values in winter and in the North might be underestimated.

2.5.2 Population size

We base the population density of our study on HYDE11 for the year AD 100 (for sources see Klein Goldewijk et al., 2011). We divided the population counts from HYDE11 (5' grid) by the gridbox area before interpolating the such derived population densities to the Gaussian grid of ECHAM-HAM-SALSA. Using this approach, the HYDE11 population size between 10° E and 50° E, 20° N and 60° N is around 55 million people (the number of people living within the political boundaries of the Roman Empire would be somewhat smaller). However, the population size of the Roman Empire is still debatable since there is disagreement what the census tallies represent. The number of HYDE11 lies in the range of the so-called "low count" scenario (Scheidel, 2008), but there are also proponents of a "middle count" and a "high count" hypothesis (Hin, 2013; Scheidel, 2008). With the "middle count" approach, Hin (2013) arrived at 6.7 million (range between 5 and 10 millions) free citizens in Italy compared to approximately 4 million with the "low count" for 28 BCE (i.e. a factor of 1.25-2.5 higher). The "high count" would result in a roughly 3 times larger population size, i.e. more than 100 million people (maybe up to 160 million) living in the whole Empire if we assume that the population densities in other parts of the Empire were similar to Italy (Scheidel, 2008, 2009).

Clim. Past Discuss., https://doi.org/10.5194/cp-2019-56
Manuscript under review for journal Clim. Past
Discussion started: 24 May 2019

Climate of the Past Discussions

Based on these different literature values, we used the estimate from HYDE11 for our low emission scenario. For the intermediate and the high emission scenarios, we decided to multiply the population densities of the HYDE database with factors of 1.5 and 2.5, respectively.

2.5.3 Aerosol emission factors

Last but not least, we needed to estimate aerosol emission factors from burning biofuel. We compiled an overview of BC, OC, and SO_2 emission measurements from different studies (Sect. S14, Table S17). Composite estimates were not considered. Note that we treated BC and elemental carbon (EC) to be the same. We grouped the measurements according to the fuel type, i.e. wood (key 1 in Table S17), agricultural waste (key 2), charcoal burning (key 5), and charcoal production (key 6). Woody agricultural waste was counted as wood. We neglected coal as a fuel type although it was widespread in Roman Britain (Smith, 1997). This is justified since the centres of the classical civilisations (especially the Mediterranean region) were not rich in coal (Malanima, 2013). A few measurements refer to PM10 (i.e. aerosol/particulate matter with aerodynamic diameters $< 10\,\mu m$) or PM4 instead of PM2.5, but the difference is usually small (a few percent between PM10 and PM2.5 in Turn et al., 1997). Similarly, we neglected the difference between SO_2 and SO_x since the latter is dominated by SO_2.

For the different sectors (i.e. wood, agricultural waste, charcoal burning, and charcoal production), we calculated a lower, an intermediate, and an upper estimate for EF after the following procedure:

- For all measurements, the mean, the standard deviation, and the number of samples N were collected.
- If N was larger than 1, but the standard deviation was not given and could not be calculated (e.g. from plots, confidence intervals, or data in the Supplementary Material), we estimated it by assuming a coefficient of variance of 50% for OC and BC and of 80% for SO_2. We assessed these coefficients of variance from all other observations providing standard deviation and mean. The samples for which the standard deviation was estimated are marked in Table S17.
- If the sample size for measurements was given as a range (e.g. "3 or 4"), we always took the lower number as N. When N was larger than 1 but not given, we assumed $N = 2$.
- Following Bond et al. (2004), we assumed that EFs follow a log-normal distribution. From the sample mean m and standard deviation s, the mean μ and the standard deviation σ of the log-normal distribution were calculated:

$$\mu = \ln\left(\frac{m^2}{\sqrt{s^2 + m^2}}\right) \tag{2}$$

$$\sigma = \sqrt{\ln\left(\frac{s^2}{m^2} + 1\right)} \tag{3}$$

- For each emission sector, we randomly drew samples from the log-normal distributions with the calculated μ and σ.
- We used three different methods how to weight the different samples: i) every measurement (in Table S17) had the same weight; ii) the measurements were weighted with N; iii) every study had the same weight (differentiated by horizontal

Clim. Past Discuss., https://doi.org/10.5194/cp-2019-56
Manuscript under review for journal Clim. Past
Discussion started: 24 May 2019

lines in Table S17). The three weighting methods can result in very different estimates, e.g. for OC emission factors from wood combustion (medians of $2.4\,\mathrm{g\,kg^{-1}}$, $0.90\,\mathrm{g\,kg^{-1}}$, and $3.0\,\mathrm{g\,kg^{-1}}$, respectively).

– From the randomly generated samples, we calculated the median and the lower and upper quartile for each weighting method (note that the median is somewhat smaller than the expected value; Bond et al., 2004). The medians of the three weighting methods were then averaged, and the same was done for the quartiles.

We considered the median to be the intermediate estimate for EF and the quartiles to be the lower and the upper estimates. We did not choose more extreme percentiles for the lower and the upper estimates because the large variability in the measurements of EF reflects the high variability in burning conditions (e.g. smouldering versus flaming), fuels, combustion devices, and measurement devices. We explicitly wanted to consider these different conditions and not only sample from one (or a few) measurements conducted under specific conditions. In general, more measurements for BC and OC than for SO_2 are available; however, since SO_2 emissions from biomass burning are small, we do not consider this to be an issue. In Sect. S4, the estimated EFs for the different sectors as well as the weighting of these different sectors are discussed. As described there, we estimate that 20% of the fuel consisted of agricultural waste, 40% of charcoal (in terms of wood that needs to be converted to charcoal), and 40% of wood. The combined aerosol emission factors were thus calculated as:

$$EF_{\mathrm{combined}} = 0.2 \cdot EF_{\mathrm{agr}} + 0.4 \cdot EF_{\mathrm{ch_w}} + 0.4 \cdot EF_{\mathrm{wood}}, \tag{4}$$

For the intermediate scenario, we inserted the medians for EF_{agr}, $EF_{\mathrm{ch_w}}$, and EF_{wood}. For the low and the high estimates, the lower and the upper quartiles were used, respectively. The values for EF_{combined} can be found in Table 1.

2.6 Aerosol emissions from crop residue burning

In the Greco-Roman world, fire was widely employed to fertilise fields, to create or regenerate pastures, to control pests, or to hunt (Ascoli and Bovio, 2013). In all simulations where we included the impact of anthropogenic aerosols, we considered the impact of humans on fires by (i) reducing the (natural) fire emissions calculated from CBALONE-SPITFIRE to account for crop and pasture areas (Sect. S3) and (ii) by estimating fire emissions from pasture and crop residue burning. In the following, we will first estimate aerosol emissions from crop residue burning before deriving estimates for pasture burning.

Next to fallow, crop rotation, and green manuring (i.e. plowing legumes in the soil; White, 1970), burning crop residues on the field was one method to increase the fertility of soils in Roman agriculture (Spurr, 1986). Since crop residues are burnt after harvest, emissions from open crop residue burning have a strong seasonal cycle (as for example shown for present-day China by Li et al., 2016a; Zhang et al., 2016). Today, harvest in the Mediterranean region takes place approximately from the beginning of May to the end of August[2], which is in accordance with summer being the time of harvest around AD 100 (Spurr, 1986). We thus spread the fire emissions from crop residue burning over these four months; we neglected that a part of the harvest might have been burnt after August due to drying in the field. Since fires can get out of control at very high

[2]http://www.claas.de/faszination-claas/themen/erntekalender-weltweit, last access: 23 August 2018

Clim. Past Discuss., https://doi.org/10.5194/cp-2019-56
Manuscript under review for journal Clim. Past
Discussion started: 24 May 2019

Climate of the Past Discussions

Table 2. The values needed to calculate the aerosol emissions from crop residue burning (Equation 5) for the low, the intermediate, and the high scenarios. Note that the total area of crop in the study domain ($\text{Area}_{\text{crop}}$) is shown instead of the fraction per gridbox (Fr_{crop}). The bold values for Y show which values were taken for the calculation, and the values in brackets represent the yields considering fallow.

Var.	Unit	Low estimate	Intermediate estimate	High estimate
Y (HYDE11)	$\text{kg}\,\text{ha}^{-1}$	**440**	**660**	1100
		(660-880)	(990-1320)	(1650-2200)
Y (KK11)	$\text{kg}\,\text{ha}^{-1}$	170	260	**430**
		(255-340)	(390-520)	(645-860)
$\text{Area}_{\text{crop}}$	$10^5\ \text{km}^2$	5.46	5.46	13.9
$Fr_{\text{crop burnt}}$	$\%\ \text{yr}^{-1}$	20	40	80
s	-	1.9	1.9	1.9
d	-	0.85	.85	0.85
p_b	-	0.87	0.74	0.56
C_f	-	0.9	0.9	0.9
EF_{crop}, BC	$\text{g}\,\text{kg}^{-1}_{\text{dry fuel}}$	0.28	0.52	0.77
EF_{crop}, OC	$\text{g}\,\text{kg}^{-1}_{\text{dry fuel}}$	1.31	2.36	4.56
EF_{crop}, SO_2	$\text{g}\,\text{kg}^{-1}_{\text{dry fuel}}$	0.095	0.29	0.53

temperatures and are unlikely to be ignited at very low temperatures (Pfeiffer et al., 2013), we assume that crop burning only occurs when the surface temperature averaged over 20 years is below 0 °C or above 30 °C. The emitted mass was shifted to the other months if there were any. The regions where temperature fell below or exceeded these thresholds were calculated offline using the surface temperature simulated with ECHAM-HAM-SALSA (without human impact).

The aerosol emission fluxes [$\text{kg}\,\text{m}^{-2}\,\text{s}^{-1}$] were calculated with the following equation (adapted from Webb et al., 2013):

$$EM_{\text{crop}} = Fr_{\text{crop}} \cdot Y \cdot d \cdot s \cdot p_b \cdot Fr_{\text{crop burnt}} \cdot C_f \cdot EF_{\text{crop}}, \tag{5}$$

where Fr_{crop} is the fraction of the total gridbox covered by crop, Y is the crop harvest fresh weight [$\text{kg}_{\text{crop}}\,\text{m}^{-2}$], d is the dry matter content of the yield [-], s is the ratio between the residue mass and the crop yield mass [$\text{kg}_{\text{residue}}\,\text{kg}_{\text{crop}}{}^{-1}$], p_b [-] is the proportion of residue which is burnt (and not used for other purposes such as fuel consumption), $Fr_{\text{crop burnt}}$ is the fraction of crop that is burnt per time [s^{-1}], C_f is the combustion factor [-], i.e. the proportion of available fuel that is actually burnt, and EF_{crop} is the emission factor of crop residue [$\text{kg}_{\text{aerosol}}\,\text{kg}^{-1}_{\text{residue}}$]. We consider low, intermediate, and high estimates for $Fr_{\text{crop burnt}}$ and EF_{crop} because these variables have high uncertainties. Since Fr_{crop}, Y, and p_b depend on the population size (below), they also have different values for the different scenarios. All values are summarised in Table 2.

2.6.1 Crop yield Y, fraction of crop Fr_{crop}, and proportion of residue burnt p_b

Cereals were the nutritional basis in the Roman Empire (Witcher, 2016) and typical yields were recorded by the agronomists of Classical Antiquity. Based on ancient sources and the work of Goodchild (2007) and Hopkins (2017), we estimated that yields representative for the whole Roman Empire are in the range between $500\,\text{kg}\,\text{ha}^{-1}$ and $1000\,\text{kg}\,\text{ha}^{-1}$ (Sect. S5).

Clim. Past Discuss., https://doi.org/10.5194/cp-2019-56
Manuscript under review for journal Clim. Past
Discussion started: 24 May 2019

It is fair to assume that the amount of crop produced scaled with the population size. Total crop production depends both on the crop area Fr_{crop} and crop yield Y. These two variables can therefore not be estimated independently. Following Kessler and Temin (2007, estimate for Rome), we assumed that around $0.8\,\mathrm{kg}$ of wheat (which was the most important nutrient) was consumed per person per day. We roughly estimated that the wheat production was around 50% higher than the wheat consumption (resulting in $1.2\,\mathrm{kg}$ of crop yield) to consider that a part of the produced crop yield was lost through, e.g. transport or insect damage (Spurr, 1986), used for fodder (Spurr, 1986), or needed for seeding (Hopkins, 1980).

For the low emissions scenario where the population size originates from HYDE11, this wheat production results in a yield of $440\,\mathrm{kg\,ha^{-1}}$ with the crop area based on HYDE11. For consistency, we use the simulated crop areas from ECHAM-HAM-SALSA (which are somewhat smaller; Sect. 2.3) for this calculation instead of the original input data. This yield is a bit lower than the estimates of crop production mentioned above (500-$1000\,\mathrm{kg\,ha^{-1}}$). However, considering that part of the crop area was used for other purposes than planting cereals or legumes (e.g. vineyards, which were not burnt) and that the crop area estimates from HYDE11 include areas that can lie fallow, the number seems reasonable: if we assume that fallow took place every second or third year (Goodchild, 2007), "actual" crop yields increase from $440\,\mathrm{kg\,ha^{-1}}$ to $\approx$ 660-$880\,\mathrm{kg\,ha^{-1}}$. For the intermediate scenario where population size is larger than in the low emission scenario, the HYDE database results in high but still reasonable estimates of crop yield ($660\,\mathrm{kg\,ha^{-1}}$; $\approx$ 990-$1320\,\mathrm{kg\,ha^{-1}}$ if fallow is considered). The high population density in the high emission scenario would require an unrealistically high crop yield when combined with the crop area of HYDE11 ($1100\,\mathrm{kg\,ha^{-1}}$; 1650-$2200\,\mathrm{kg\,ha^{-1}}$ with fallow). When using the KK11 land use reconstruction, which has a much larger crop area, the needed crop yield would be $430\,\mathrm{kg\,ha^{-1}}$ ($\approx$ 645-$860\,\mathrm{kg\,ha^{-1}}$), which is regarded as realistic. Therefore, the HYDE11 land use is chosen for the low and the intermediate scenarios while KK11 is chosen for the high scenario.

For the yields, we took the values mentioned above (Table 2), which are calculated based on the crop area and the population size, for our calculations.

In Sect. 2.5, we assumed that 20% of the fuel consisted of agricultural waste. Therefore, we should account for the fact that the higher the assumed population in our scenarios, the more crop residue is taken from the field. On the one hand, part of this agricultural waste used as fuel consisted not of cereal crop residue but e.g. of dung or olive pits, which speaks for a larger p_b. On the other hand, also other purposes of crop residue than fuel depend directly on the population density, e.g. the residue mass that was used for construction purposes or for filling mattresses (Spurr, 1986), which speaks for a lower p_b. Here we simply assume that the crop residue taken from the field per person is equal to 20% of the consumed fuel mass, and thus arrive at $p_b = 0.87$, $p_b = 0.74$, and $p_b = 0.56$ for the low, the intermediate, and the high scenarios, respectively.

2.6.2 Fraction of crop burnt $Fr_{\mathrm{crop\ burnt}}$

Part of the remaining residue on the field was burnt. We estimate this fraction in Sect. S6 while assuming that the fraction of residue burnt in the field did not depend on the remaining residue mass per area but rather on cultural practices. We used present-day estimates from developing countries as an indication. Based on cultural practices, we estimate (details in Sect. S7) that roughly 40% of the crop area is annually burnt for the intermediate emission scenario ($Fr_{\mathrm{crop\ burnt}} = 0.4\,\mathrm{yr^{-1}}$). For the low and the high emission scenarios, we changed this fraction by a factor of 2 and arrive at 20% and 80%, respectively. Note

Clim. Past Discuss., https://doi.org/10.5194/cp-2019-56
Manuscript under review for journal Clim. Past
Discussion started: 24 May 2019

Table 3. The values used to calculate the aerosol emissions from pasture burning (Equation 6) for the low, the intermediate, and the high scenarios. Note that the total area of pasture in the study domain ($\text{Area}_{\text{pasture}}$) is shown instead of the fraction per gridbox (Fr_{pasture}).

Var.	Unit	Low estimate	Intermediate estimate	High estimate
$\text{Area}_{\text{pasture}}$	$10^5\ \text{km}^2$	4.75	4.75	13.9
$Fr_{\text{pasture burnt}}$	$\%\,\text{yr}^{-1}$	15	30	60
F	$\text{kg}\,\text{m}^{-2}$	0.35	0.35	0.35
EF_{pasture}, BC	$\text{g}\,\text{kg}^{-1}_{\text{dry fuel}}$	0.48	0.62	0.81
EF_{pasture}, OC	$\text{g}\,\text{kg}^{-1}_{\text{dry fuel}}$	4.85	6.64	7.68
EF_{pasture}, SO_2	$\text{g}\,\text{kg}^{-1}_{\text{dry fuel}}$	0.31	0.41	0.53

that fallow as well as the part of the residue taken from the field for fuel combustion are already accounted for in p_b and the derivation of Y.

2.6.3 Other variables in Equation 5

Modern values of the harvest index (= the ratio of grain yield to the total plant mass) for wheat range between 0.4 and 0.6 (Hay, 1995). The harvest index was typically lower (around 0.3) at the end of the nineteenth century (Hay, 1995; Sinclair, 1998), but the sometimes exceptionally high yields in ancient times could indicate that the harvest index might have been higher at this time (Sinclair, 1998). For all simulations, we used a harvest index of 0.35, which corresponds to $s = 1.9$. Following Webb et al. (2013), we chose $d = 0.85$ and $C_f = 0.9$. The emission factors for burning of crop residues on the field were estimated using the same method as described in Sect. 2.5.3 using values from Table S17 (key 3).

2.7 Aerosol emissions from pasture burning

According to the agronomist Columella (who lived in the first century AD), pasture from long fallow was burnt in late summer to achieve more tender growth (Spurr, 1986). Based on Aalde et al. (2006, Equation 2.27), we calculated the aerosol emission fluxes [$\text{kg}\,\text{m}^{-2}\,\text{s}^{-1}$] with:

$$EM_{\text{pasture}} = Fr_{\text{pasture}} \cdot Fr_{\text{pasture burnt}} \cdot F \cdot EF_{\text{pasture}}, \tag{6}$$

where Fr_{pasture} is the fraction of the total gridbox covered by pasture, $Fr_{\text{pasture burnt}}$ is the fraction of pasture that is burnt per time [s^{-1}], F stands for fuel biomass consumption [i.e. the amount of fuel that is actually burnt; $\text{kg}_{\text{dry matter}}\,\text{m}^{-2}$], and EF_{pasture} is the emission factor of pasture burning [$\text{kg}_{\text{aerosol}}\,\text{kg}^{-1}_{\text{dry matter}}$]. In accordance with the crop residue burning emissions, we used the land cover reconstructions from HYDE11 for the low and the intermediate scenarios and the land cover estimates from KK11 for the high emission scenario. We considered low, intermediate, and high estimates for $Fr_{\text{pasture burnt}}$ and emission factors because these variables have large uncertainties.

Clim. Past Discuss., https://doi.org/10.5194/cp-2019-56
Manuscript under review for journal Clim. Past
Discussion started: 24 May 2019

2.7.1 Fuel biomass consumption F

The increase in European grassland productivity over the last decades has been small compared to crop (Smit et al., 2008). The spatial variability of grassland productivity is quite large within Europe, ranging from $\approx 0.15\,\mathrm{kg\,m^{-2}\,yr^{-1}}$ in the Mediterranean region up to $0.65\,\mathrm{kg\,m^{-2}\,yr^{-1}}$ in the Atlantic zones; the median over the different climate zones of Europe is $0.33\,\mathrm{kg\,m^{-2}\,yr^{-1}}$ (Smit et al., 2008). As a consequence, we expect that also the fuel load and the fuel biomass consumption show spatial variability. In contrast to fuel biomass consumption, fuel load refers to fuel that is available (but not necessarily burnt) and often refers to aboveground biomass only. Nevertheless, values for fuel biomass consumption and fuel load are quite comparable because grass easily burns and mainly aboveground biomass is consumed during pasture burning. Based on different studies that measured fuel load and fuel biomass consumption (Sect. S7), we roughly estimate that the fuel biomass consumption is $F = 0.35\,\mathrm{kg_{dry\ matter}\,m^{-2}}$.

2.7.2 Fraction of pasture burnt $Fr_{\mathrm{pasture\ burnt}}$

In the Mediterranean region, pasture burning has continued throughout history to the present day and is one component that has shaped the diversity of Mediterranean landscapes as we know them (Montiel and Kraus, 2010). In temperate and boreal Europe, the burning of grasslands for pasture was common on lands which were too poor in nutrients for agriculture, e.g. heathlands (Montiel and Kraus, 2010). In Sect. S8 we summarise guidelines for the rate of prescribed burning from different regions around the world. Based on this literature and accounting for regional variability, we assumed that $30\,\%$ of the pasture area is burnt per year, which corresponds to burning roughly every 3 years. For the low and the high emission scenarios, we changed this fraction by a factor of 2 and arrive at $15\,\%$ and $60\,\%$, respectively. We assumed that the aerosols from pasture burning were emitted throughout the year, but – like for crop residue – that no pasture was burnt in months which are very cold or hot (monthly average temperatures below $0\,^{\circ}\mathrm{C}$ or above $30\,^{\circ}\mathrm{C}$).

2.7.3 Emission factor EF_{pasture}

Using the method described in Sect. 2.5.3 and the measurements from Table S17 (key 4), the emission factors in Table 3 were derived. We again used the lower quartiles for the low, the medians for intermediate, and the upper quartiles for high emission scenarios.

2.8 Simulations

We conducted six time-slice experiments for AD 100 (Table 4): no_human, LCC_HYDE, LCC_KK, LCC_HYDE_low, LCC_HYDE_int, and LCC_KK_high. The simulation no_human does not account for anthropogenic impacts (except for potential influences on greenhouse gas concentrations at this time). LCC_HYDE and LCC_KK consider only the effects of anthropogenic land cover change (Sect. 2.3) on climate. The simulations LCC_HYDE_low, LCC_HYDE_int, and LCC_KK_high consider, in addition to anthropogenic land cover change, anthropogenic aerosol emissions due to fuel consumption, crop residue burning, and pasture burning. While the anthropogenic land cover reconstructions provide global values and are thus applied on the global

Clim. Past Discuss., https://doi.org/10.5194/cp-2019-56
Manuscript under review for journal Clim. Past
Discussion started: 24 May 2019

Climate of the Past Discussions

Table 4. Overview of the different simulations. Note that the anthropogenic land cover change is applied in ECHAM-HAM-SALSA, but not in CBALONE-SPITFIRE, which was used to calculate aerosol emissions from natural fires exclusively.

Simulation	Anthropogenic land cover	Anthropogenic aerosol emissions
no_human	-	-
LCC_HYDE	HYDE11[a]	-
LCC_KK	KK11[b]	-
LCC_HYDE_low	HYDE11[a]	low estimate[c]
LCC_HYDE_int	HYDE11[a]	intermediate estimate[c]
LCC_KK_high	KK11[b]	high estimate[c]

[a]Klein Goldewijk et al. (2011)
[b]Kaplan et al. (2011, 2012)
[c]This study; Sects. 2.5, 2.6, 2.7

scale, we only calculated anthropogenic aerosol emissions for the Roman Empire and not for other parts of the world, i.e. no anthropogenic aerosol emissions occur outside of our study domain.

The simulations have a spatial resolution of approximately $1.875° \times 1.875°$ and 47 vertical levels (T63L47). After the first three months of spin-up, natural vegetation was replaced by the area of anthropogenic land cover for AD 100 within one model year; after that the vegetation fractions were kept constant. One year of model spin-up was added after the transition to anthropogenic land cover was completed, resulting in a total spin-up of 2 years and three months. The spin-up is relatively short since we use neither an interactive ocean nor dynamic vegetation. The simulations (excluding spin-up) are 20 years long and should be representative for approximately AD 100, i.e. the time of interest.

In the standard ECHAM-HAM-SALSA version, the cloud droplet number concentration in a cloud cannot be lower than $40\,\mathrm{cm}^{-3}$ (or optionally $10\,\mathrm{cm}^{-3}$; Tegen et al., 2019). For all simulations of this study, this minimum CDNC was lowered from $40\,\mathrm{cm}^{-3}$ to $1\,\mathrm{cm}^{-3}$ (and the model was retuned) because the aerosol concentrations – and therefore most likely CDNCs – were considerably lower in AD 100 than today.

3 Results

3.1 Climate impact of anthropogenic land cover change

The simulations LCC_HYDE and LCC_KK were compared with the simulation no_human to quantify the impact of anthropogenic land cover change on climate (Tables S8, S9).

Clim. Past Discuss., https://doi.org/10.5194/cp-2019-56
Manuscript under review for journal Clim. Past
Discussion started: 24 May 2019

The replacement of natural vegetation by crop and pasture leads to a decrease in SOA precursors, which is most likely responsible for the significant[3] changes in CDNC, LWP, and CRE for LCC_KK (all cloud properties are gridmean). The changes in CRE are expected to induce a warming, but are relatively small.

Since the anthropogenic land cover changes include replacing forests with less rough vegetation types, the annual mean wind velocity at $10\,\mathrm{m}$ altitude increases averaged over our entire study domain (Table 5) when considering land use changes. The surface albedo can either increase or decrease significantly depending on the season and the region. Deforestation can introduce brighter vegetation types and thus an increase in surface albedo. However, especially after harvest crop has a smaller canopy area fraction than natural vegetation. Thus, more of the soil, which can be darker than the natural vegetation, is exposed to radiation. As a consequence, the annually averaged surface albedo decreases in parts of Europe (Fig. 1a,b) because the surface albedo there increases in summer but decreases in other seasons (not shown).

Land cover change also alters latent heat (LH) and sensible heat (SH) fluxes. The annual mean evaporative fraction (Evap_frac$=\frac{\mathrm{LH}}{\mathrm{SH+LH}}$; only calculated if both SH and LH are upward fluxes) shows regionally no significant changes (Table 5; Fig. 1c,d). In contrast, regional changes in the annual mean turbulent flux ($\mathrm{F_{turb}} = \mathrm{SH} + \mathrm{LH}$; only calculated if both SH and LH are upward fluxes) are significant and important since they are mainly responsible for regional changes in surface temperature, as can be seen in Fig. 1. In regions where the surface temperature increases significantly (parts of North Africa and Middle East), the turbulent fluxes decrease, which leads to a less efficient heat transport from the surface to the atmosphere. The natural vegetation in no_human consists mainly of raingreen shrubs and C3 grass in these regions. Averaged over our study domain, the land surface temperature increases by $0.10\,\mathrm{K}$ for LCC_HYDE (insignificant) and by $0.15\,\mathrm{K}$ for LCC_KK (significant).

Overall, the impact of anthropogenic land cover on climate is small, showing only localised warming for LCC_KK. The impact of land use in Smith et al. (2016) is much more pronounced than in our study and the changes induce a distinct cooling over Europe ($0.58\,\mathrm{K}$), which is stronger in summer than in winter. The setup of their simulations is considerably different from ours; as an example, their model HadCM3 is coupled with an ocean model, whereas we prescribe SST and SIC. However, we think that the large differences are mainly caused by the vegetation or atmospheric models. Intercomparison studies have shown that not all models agree on the sign of annual mean temperature changes induced by deforestation over North America and in mid-latitudes (Lejeune et al., 2017; Winckler et al., 2018). Satellite studies indicate that the impact of deforestation shifts from a warming in the tropics to a cooling in boreal regions, but the latitude where this shift occurs is somewhat uncertain: while Li et al. (2015) found that this transition zone lies between $35°$ and $45°$ N, Li et al. (2016c) state that it is at approximately $50°$ N. In our simulations, significant warming occurs south of $40°$ N, which is in qualitative agreement with these present-day observations. However, nearly no significant temperature changes occur in Europe in our simulations. In contrast to our findings the results by Strandberg and Kjellström (2019), which are based on regional modelling under present-day conditions, suggest that biogeophysical effects related to deforestation lead to a warming in most parts of Europe due to reduced evapotranspiration.

[3]The paired t-test was used. We chose a paired test since the natural fire emissions have the same interannual pattern across all simulations. The effect of multiple hypothesis testing was considered by controlling the false discovery rate as described in Wilks (2016) using $\alpha_{\mathrm{FDR}} = 2 \cdot \alpha$.

Clim. Past Discuss., https://doi.org/10.5194/cp-2019-56
Manuscript under review for journal Clim. Past
Discussion started: 24 May 2019

Climate of the Past Discussions
Open Access
EGU

Table 5. The impact of anthropogenic land cover change on different variables: horizontal wind velocity at 10 m, surface albedo over land, evaporative fraction, turbulent flux, and land surface temperature. Shown are values for the simulation without anthropogenic land cover (no_human) and simulations including anthropogenic land cover (LCC_HYDE and LCC_KK). The values are annual means and averaged from 10° W to 50° E and from 20° N to 60° N. Changes with respect to no_human are shown in brackets and the stars indicate changes that are significant (5% significance level; $N = 20$). Absolute changes are given for T_s and relative changes for all other variables.

Var.	Unit	no_human	HYDE11		KK11	
$Wind_{10}$	$m\,s^{-1}$	4.27	4.30	$(+0.9\%)*$	4.41	$(+3.3\%)*$
Albedo	-	0.26	0.26	(-0.1%)	0.26	$(+0.1\%)$
Evap_frac	-	0.36	0.36	$(+0.8\%)$	0.36	$(+1.6\%)*$
F_{turb}	$W\,m^{-2}$	71.78	71.91	$(+0.2\%)$	71.99	$(+0.3\%)$
T_s	K	290.14	290.25	$(+0.10)$	290.30	$(+0.15)*$

Clim. Past Discuss., https://doi.org/10.5194/cp-2019-56
Manuscript under review for journal Clim. Past
Discussion started: 24 May 2019

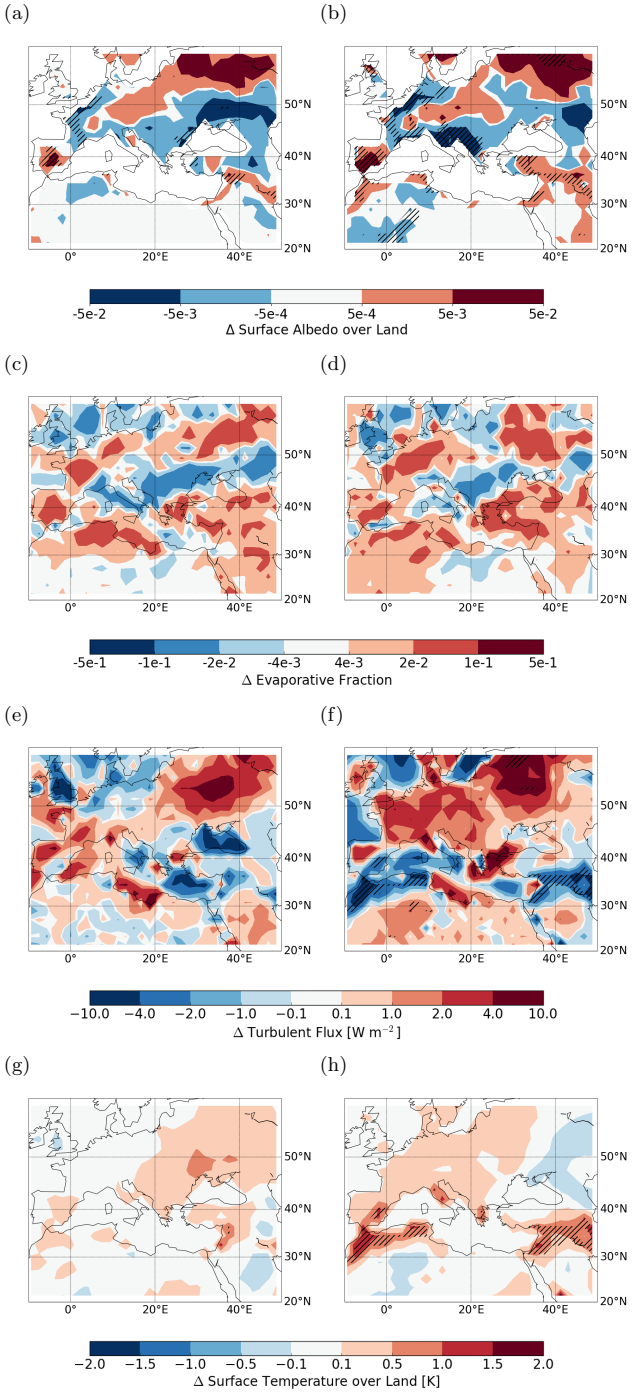

Figure 1. The impact of anthropogenic land cover change on climate using HYDE11 (left) and KK11 (right). Shown are changes in surface albedo over land (a,b), evaporative fraction (c,d), turbulent flux (e,f), and land surface temperature (g,h). Statistically significant changes (5% significance level; $N = 20$) are hatched.

Clim. Past Discuss., https://doi.org/10.5194/cp-2019-56
Manuscript under review for journal Clim. Past
Discussion started: 24 May 2019

3.2 Impact of anthropogenic aerosol emissions in AD 100 on climate and PM2.5 concentrations

Our calculated anthropogenic aerosol emissions for AD 100 are compared with the anthropogenic emissions estimate for AD 1850 in Sect. S10. Furthermore, the simulated natural fire emissions for AD 100 are compared to the anthropogenic aerosol emissions in Sect. S11; this gives a first indication of the potential impact of the latter. In this section, the influence of anthropogenic aerosol emissions (AD 100) on climate is assessed by comparing simulations considering anthropogenic land cover change and aerosol emissions with simulations that only consider anthropogenic land cover change (i.e. LCC_HYDE_low/LCC_HYDE_int compared with LCC_HYDE; LCC_KK_high compared with LCC_KK). The changes in the most important variables, averaged over the study domain and the whole year, are shown in Table 6. Tables S10, S11, and S12 include more variables and show also seasonal averages for the low, the intermediate, and the high emission scenarios, respectively.

The BC and OC burdens (= vertically integrated mass) change significantly for all emission scenarios (Tables S10 to S12), with stronger changes for BC, whereas the SO_4 burden does not change significantly. This is due to the different emission sectors of the three aerosol types: while fire emissions are the only natural source of BC particles, OM also has biogenic sources, and SO_4 predominantly forms from gas-to-particle conversion of volcanic and oceanic precursor emissions. The changes in aerosol burdens show large seasonal differences: in summer, the BC and OC burdens decrease for the low and the intermediate emission scenarios because of the reduction in natural fires (Sect. S11). In winter, the BC and OC burdens increase pronouncedly for all emission scenarios due to anthropogenic aerosol emissions.

Averaged over the study domain and the year, ARE changes by $0.06\,\mathrm{W\,m^{-2}}$, $0.12\,\mathrm{W\,m^{-2}}$, and $0.12\,\mathrm{W\,m^{-2}}$ for the low, the intermediate, and the high emission scenarios, respectively (Table 6). Largest increases occur over North Africa and Europe (Fig. 2a-c). In contrast to ARE, the changes in CRE are negative and considerably more pronounced: $-2.11\,\mathrm{W\,m^{-2}}$, $-4.17\,\mathrm{W\,m^{-2}}$, and $-7.63\,\mathrm{W\,m^{-2}}$ for the three scenarios, respectively. The changes predominantly occur over Europe (Fig. 2d-f). The cooling effect of clouds is enhanced because they become optically thicker and more abundant due to aerosol-induced increases in CDNC and LWP (Tables S10 to S12).

Since the negative changes in CRE are larger than the positive changes in ARE, the land surface temperature over Europe decreases for all scenarios (Fig. 2g-i). Averaged over the study domain, the temperature decreases significantly by $-0.17\,\mathrm{K}$, $-0.23\,\mathrm{K}$, and $-0.46\,\mathrm{K}$ for the three scenarios, respectively.

Aerosol particles are also relevant because of their impact on human health. According to Makra (2015), air pollution had substantial consequences in cities in ancient times. As an example, the philosopher Seneca wrote that he needed to leave Rome in order to escape the smoke and the kitchen smells and to feel better (Makra, 2015). As maintained by the World Health Organisation (WHO; 2006), the annual mean PM2.5 concentration should not exceed $10\,\mathrm{\mu g\,m^{-3}}$. Figure 3 shows the background surface PM2.5 concentrations as well as the increases due to the anthropogenic emissions. For the low emission scenario, changes in the PM2.5 concentration are below $1\,\mathrm{\mu g\,m^{-3}}$ everywhere. For the intermediate emission scenario, significant increases mainly range between 0.1 and $2\,\mathrm{\mu g\,m^{-3}}$, which is for most places insufficient to increase the background concentrations to values above $10\,\mathrm{\mu g\,m^{-3}}$. Only for the high emission scenario are the increases in PM2.5 concentration pronounced enough

Clim. Past Discuss., https://doi.org/10.5194/cp-2019-56
Manuscript under review for journal Clim. Past
Discussion started: 24 May 2019

Climate of the Past Discussions
Open Access
EGU

Table 6. Annual mean impact of anthropogenic aerosol emissions on different variables averaged over the study domain (10° W to 50° E and 20° N to 60° N): cloud droplet number concentration (CDNC), liquid water path (LWP), cloud cover (CC), aerosol radiative effect (ARE), cloud radiative effect (CRE), and land surface temperature (T_s) for all simulations except no_human. Significant (5% significance level; $N = 20$) changes compared to the respective reference are marked with '*'. Absolute changes are given for T_s and relative changes for all other variables. [1]: Changes are relative to HYDE11. [2]: Changes are relative to KK11.

Var.	Unit	HYDE11	KK11	low[1]		int[1]		high[2]	
CDNC	$10^9\,\mathrm{m}^{-2}$	22.87	21.90	26.12	(+14.2%)*	32.76	(+43.2%)*	58.34	(+166.4%)*
LWP	$\mathrm{g\,m}^{-2}$	47.64	45.98	56.69	(+19.0%)*	66.97	(+40.6%)*	84.47	(+84.1%)*
CC	-	0.48	0.48	0.50	(+2.7%)*	0.50	(+4.2%)*	0.52	(+8.7%)*
ARE	$\mathrm{W\,m}^{-2}$	−0.66	−0.64	−0.60	(−9.0%)*	−0.54	(−18.0%)*	−0.52	(−18.7%)*
CRE	$\mathrm{W\,m}^{-2}$	−8.83	−8.58	−10.95	(+23.9%)*	−13.01	(+47.2%)*	−16.21	(+88.9%)*
T_s	K	290.25	290.30	290.07	(−0.17)*	290.02	(−0.23)*	289.84	(−0.46)*

to exceed the WHO threshold in some regions (e.g. Algeria, Egypt). Note that the maximum PM2.5 concentrations are to some degree underestimated due to our coarse model resolution. As an example, Li et al. (2016b) found that the maximum simulated PM2.5 concentrations decrease by -21% if the resolution decreases from $0.5° \times 0.66°$ to $2° \times 2.5°$.

Clim. Past Discuss., https://doi.org/10.5194/cp-2019-56
Manuscript under review for journal Clim. Past
Discussion started: 24 May 2019

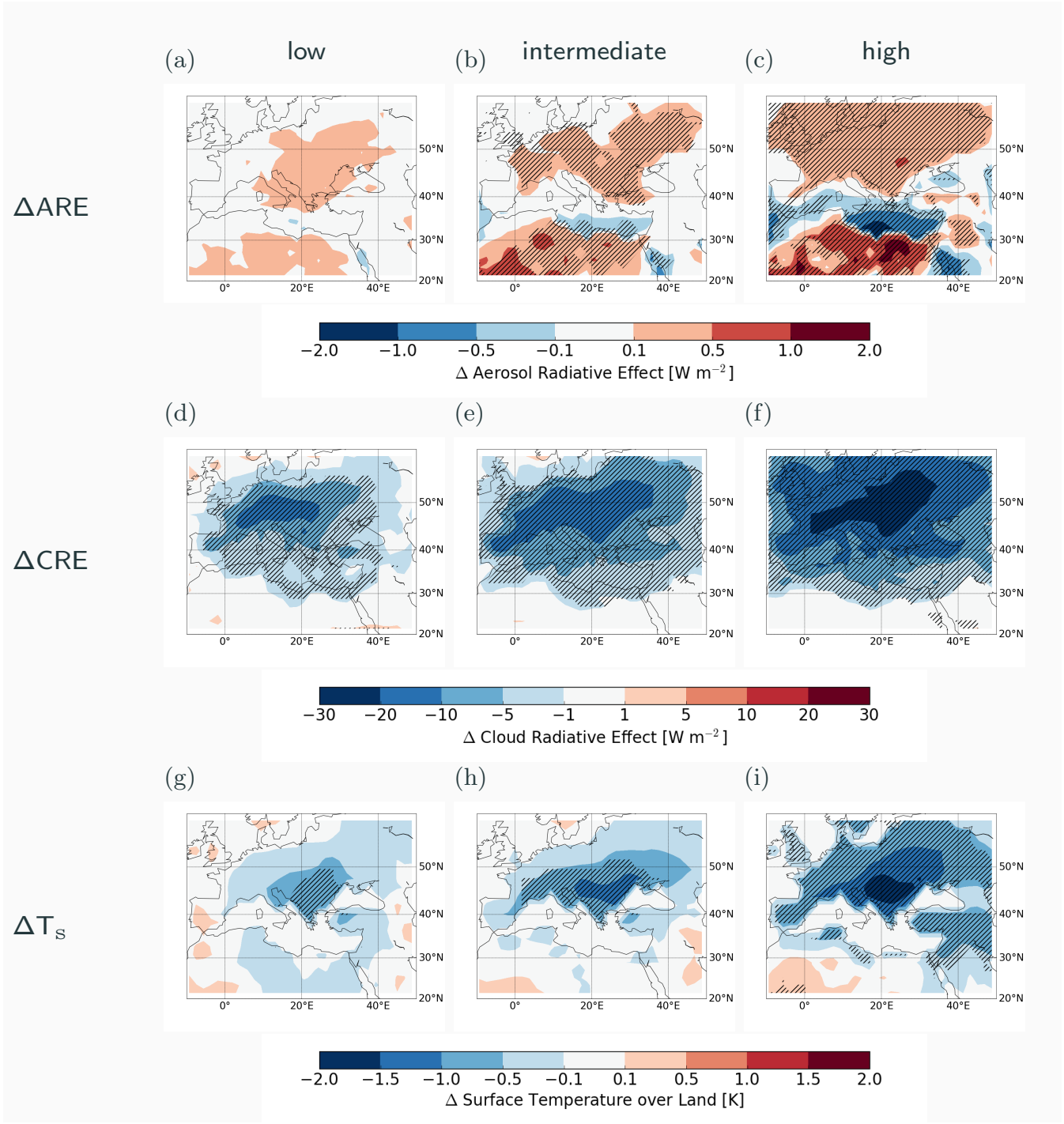

Figure 2. The impact of anthropogenic aerosol emissions for the low (left), the intermediate (middle), and the high emission scenarios (right). Shown are differences in aerosol radiative effect (top), cloud radiative effect (middle), and land surface temperature (bottom). Statistically significant changes (5% significance level; $N = 20$) are hatched.

Clim. Past Discuss., https://doi.org/10.5194/cp-2019-56
Manuscript under review for journal Clim. Past
Discussion started: 24 May 2019

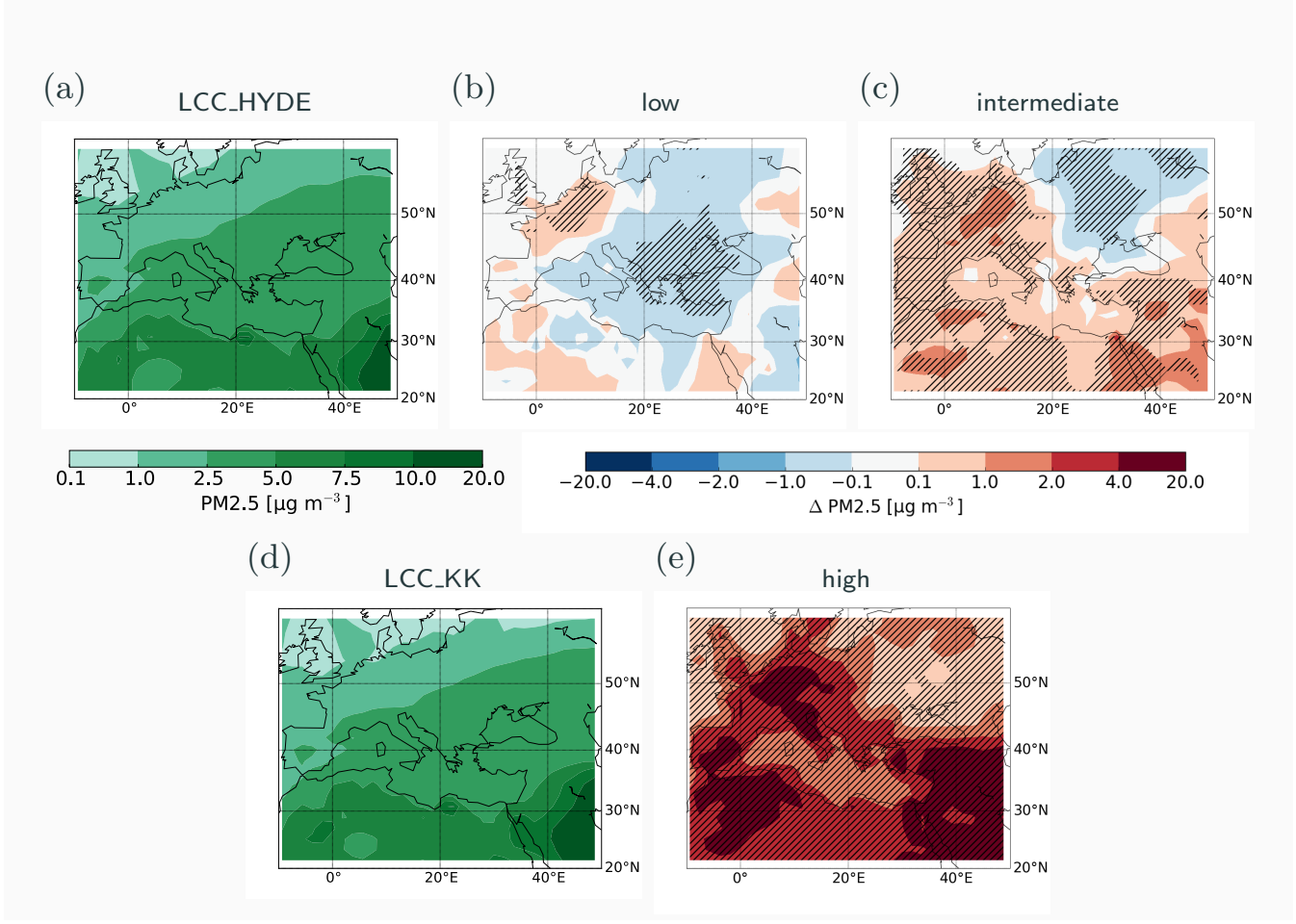

Figure 3. The background surface PM2.5 concentrations (a: LCC_HYDE; d: LCC_KK) and the changes in PM2.5 surface concentrations due to anthropogenic aerosol emissions for the low (b; LCC_HYDE_low), the intermediate (c; LCC_HYDE_int), and the high (e; LCC_KK_high) emission scenarios. Statistically significant changes (5% significance level; $N = 20$) are hatched.

Clim. Past Discuss., https://doi.org/10.5194/cp-2019-56
Manuscript under review for journal Clim. Past
Discussion started: 24 May 2019

Climate of the Past Discussions
Open Access
EGU

Table 7. The impact of anthropogenic land cover change and aerosol emissions on land surface temperature. Shown are values for the reference simulation without anthropogenic land cover change and aerosol emissions (no_human) and for the simulations with both anthropogenic land cover change and aerosol emissions (LCC_HYDE_low, LCC_HYDE_int, and LCC_KK_high). The values are annual means and averaged from 10° W to 50° E and from 20° N to 60° N. Absolute differences are shown in brackets, and stars indicate changes that are significant (5% significance level; $N = 20$).

Var.	Unit	no_human	low		int		high	
T_s	K	290.14	290.07	(−0.07)	290.02	(−0.13)	289.84	(−0.31)∗

3.3 Combined climate impact of anthropogenic land cover change and aerosol emissions

To assess the combined effect of anthropogenic land cover change and aerosol emissions, the simulations LCC_HYDE_low, LCC_HYDE_int, and LCC_KK_high are compared with the simulation no_human. While the warming induced by land cover change occurs in North Africa and the Middle East (Fig. 1g,h), the aerosol-induced cooling is strongest over Central and Eastern Europe (Fig. 2g,h,i). Being the sum of these changes, the changes in surface temperature for the combined effect (Fig. 4a,b,c) show the same features, namely a cooling over Europe and a warming over parts of North Africa and the Middle East. However, changes are only significant for LCC_KK_high (Fig. 4c). Averaged over the study domain, the aerosol-induced cooling is stronger than the land use-induced warming, thus the land surface temperature decreases for all scenarios (Table 7), but only significantly for LCC_KK_high (−0.31 K).

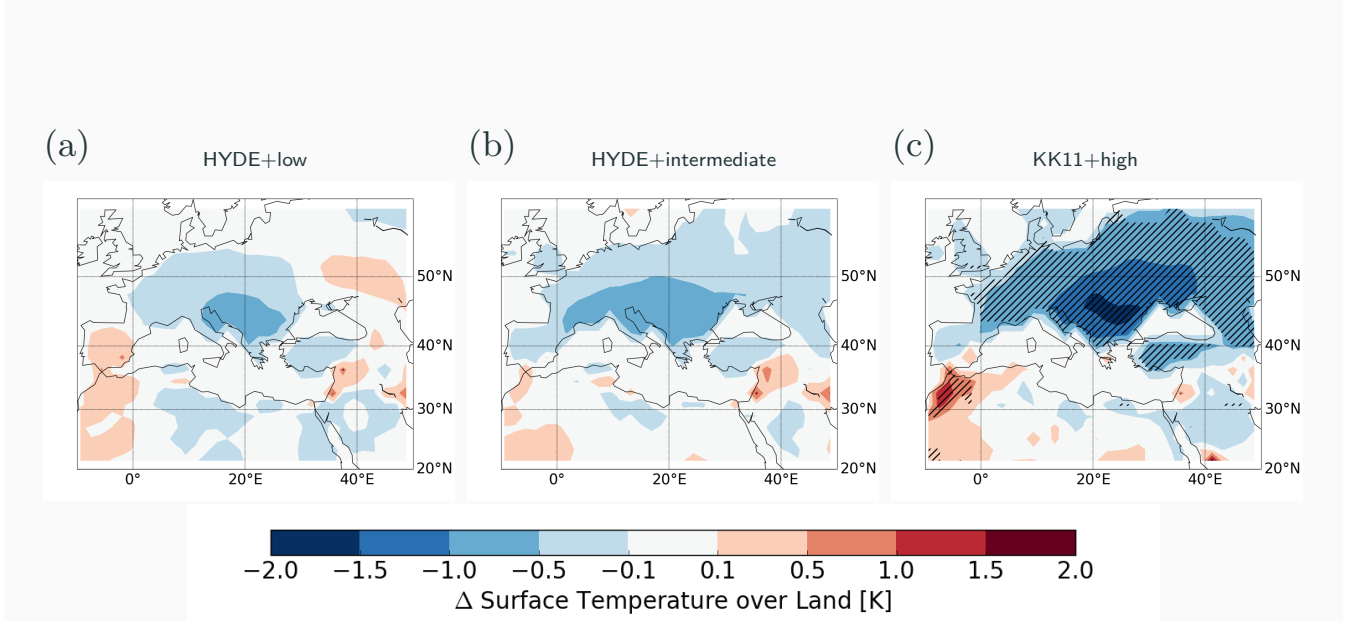

Figure 4. The impact of both anthropogenic land cover change and aerosol emissions on land surface temperature for the low (left), the intermediate (middle), and the high emission scenarios (right). Statistically significant changes (5% significance level; $N = 20$) are hatched.

Clim. Past Discuss., https://doi.org/10.5194/cp-2019-56
Manuscript under review for journal Clim. Past
Discussion started: 24 May 2019

4 Uncertainties and limitations

Because ECHAM-HAM-SALSA is an atmosphere-only model, SSTs and SIC were prescribed. Therefore, temperature and precipitation do not react to a perturbation as much as with an interactive ocean, implying that, in the absence of attenuating feedbacks, our simulated changes in temperature and precipitation should be underestimated. We repeated two of the simulations (no_human, LCC_HYDE_int) with a mixed-layer ocean model ($\approx$ 50 years, half of it model spin-up), and arrived indeed at larger changes in surface temperature (5 times stronger decrease in surface temperature).

The two land cover reconstructions that we chose differ widely and thus provide a measure for uncertainty. However, also the soil albedo and vegetation cover of the simulation no_human, which have a strong influence on the climate response, are subject to uncertainty. We found that the contribution of grasslands to the natural vegetation is quite high in our simulations. As an example, grasslands and tundra contribute $\approx 45\%$ to the natural vegetation between $0°$ E and $30°$ E and $30°$ N and $60°$ N. If the forest fraction were underestimated in our simulation, the impact of the anthropogenic land cover change would likely also be underestimated. This would especially be the case for creating pasture, since grasslands are preferentially converted to pasture in the model (Reick et al., 2013). Furthermore, the crop phenology of JSBACH, which considers both winter and summer crop, allows two harvests of summer crops during one year in the extratropics depending on the heat sum. Generally, the productivity of crops was smaller in the Roman Empire than today, with fallow every two to three years. The number of harvests is thus likely overestimated in JSBACH (but not in the offline calculated crop residue burning emissions), which affects for example changes in surface albedo (which could be more positive in reality).

The anthropogenic aerosol emissions that we calculated are only rough estimates. To calculate aerosol emission factors for fuel consumption, we used measurements from present-day fireplaces and traditional stoves. The measurements show a large variability, which is caused e.g. by the fuel moisture, the burning device, the fire conditions (flaming versus smouldering), or the instrumental setup. To account for the large range of observed emission factors, we considered many measurements. Nevertheless, we cannot rule out that typical stoves used in the Roman Empire had systematically different emission factors than the majority of burning devices that we considered. Another simplification is our lack of spatial variations: for many variables, we estimated one "typical" value for the whole Roman Empire. Furthermore, the uncertainties of important parameters such as population size are considerable when going so far back in time. The emissions are thus highly uncertain, and it is extremely challenging to quantitatively verify them with palaeo records. At least there is indirect evidence for aerosol emissions associated with fuel consumption and agricultural burning: marble turned grey in antique towns due to smoke, and laws were introduced against air pollution (Makra, 2015). Moreover, pollen and charcoal records show high positive correlations between fire and crops, weeds, and shrubs in Mediterranean and temperate regions in and around the Alps between 2300 BC and 800 AD (Tinner et al., 2005, 2009). Palaeo records further suggest that controlled burning was used to introduce and establish sweet chestnut in some regions (Morales-Molino et al., 2015).

The impact of our simulated anthropogenic aerosol emissions on climate strongly depends on the natural background and its seasonality. In our simulations, oceanic DMS concentrations, dust potential sources, and volcanic tropospheric SO_2 emissions are representative for present-day conditions, which could have an impact on the background aerosol concentrations. Moreover,

Clim. Past Discuss., https://doi.org/10.5194/cp-2019-56
Manuscript under review for journal Clim. Past
Discussion started: 24 May 2019

fire models show large differences, and thus it is unclear how realistic the fire emissions and the strong seasonal cycle of our CBALONE-SPITFIRE simulations (Sect. S11) are. The fire emissions from our simulations are one order of magnitude higher than the emissions by van Marle et al. (2017) in the study domain (Sect. S13), indicating that our natural fire emissions could be overestimated. On the one hand, this could indiciate that our background aerosol concentration is potentially overestimated as well. On the other hand, our model neglects pure biogenic aerosol nucleation and nitrate aerosols. Using the GLOMAP model, Gordon et al. (2016) have shown that the global annual mean CCN concentration (at 0.2% supersaturation and at cloud base level) was 12% higher in the pre-industrial atmosphere when pure biogenic nucleation is considered. The effect is not the same over the year since terpene emissions are larger in summer (Gordon et al., 2016). Therefore, our simulated background concentration when we see the highest impact of anthropogenic aerosols (winter, spring) might not be affected too much by the neglect of biogenic nucleation. In contrast, fine-mode nitrate concentrations are usually higher in winter than in summer at the present-day (Schaap et al., 2004). Assessing the impact of nitrate aerosols on climate before the occurrence of large anthropogenic emissions is challenging since ammonium nitrate aerosols only form if sulfate aerosols are neutralised and there is still ammonia left (Forster et al., 2007). Therefore, the contribution of nitrate to total aerosols depends strongly on sulfate and nitrate precursor as well as on ammonia emissions; all of these emissions have considerably increased since the pre-industrial due to anthropogenic activities (Tsigaridis et al., 2006; Hauglustaine et al., 2014). Under present-day conditions, fine-mode nitrate surface concentrations are high mainly in urban regions, while concentrations in rural areas and over the ocean are low (Malm et al., 2004; Bauer et al., 2007).

The aerosol background does not only depend on emissions, but also on other parameters such as the simulated size distribution or the calculation of removal processes. A simplification of our study is that most of the tropospheric chemistry is not calculated, hence we prescribe the oxidants that are important for the sulfur chemistry and the SOA formation. Also the vertical distribution of the aerosol particles is important when their effect on radiation and clouds is analysed. In ECHAM-HAM, vertical mixing is strong in the lower troposphere (Veira et al., 2015), and thus the anthropogenic aerosol particles emitted near the surface can easily reach altitudes where clouds form. If this vertical mixing were overestimated in the model, then the aerosol-cloud interactions would likely be overestimated as well.

Last but not least, aerosol-radiation and aerosol-cloud interactions from aerosol-climate models are uncertain. As an example, some studies show that the models typically overestimate the effect of aerosols on the cloud liquid water content, at least in some regions (Bender et al., 2018). The aerosol effective radiative forcing also depends on the minimum CDNC value (Hoose et al., 2009); since we lowered the minimum CDNC to $1\,\mathrm{cm}^{-3}$, the aerosols have a stronger impact on radiation than with the standard setup of ECHAM-HAM-SALSA where the minimum CDNC is $40\,\mathrm{cm}^{-3}$. We conducted additional simulations showing that the total ERF due to aerosols between AD 1850 and AD 2000 is $\approx -2.4\,\mathrm{W\,m}^{-2}$ with our decreased minimum CDNC value. Our $\mathrm{ERF}_{\mathrm{ari+aci}}$ thus lies at the lower end of model estimates and is outside the range of IPCC's expert judgment (-1.9 to $-0.1\,\mathrm{W\,m}^{-2}$; Boucher et al., 2013).

Clim. Past Discuss., https://doi.org/10.5194/cp-2019-56
Manuscript under review for journal Clim. Past
Discussion started: 24 May 2019

5 Conclusions

In this study, we quantified the anthropogenic influence on climate in the Roman Empire around AD 100 using an aerosol-enabled global climate model. We considered both anthropogenic land cover change and aerosol emissions. Our hypothesis was that these anthropogenic activities already at this time had a noticeable influence on climate on a continental scale. This hypothesis could be confirmed with the results we simulated as both anthropogenic land cover change and aerosol emissions induce significant surface temperature changes in some of the scenarios.

In contrast to Smith et al. (2016), who found a pronounced cooling induced by anthropogenic land cover change over Europe, land surface temperature increases in our simulations. The anthropogenic land cover reconstruction based on HYDE (Klein Goldewijk et al., 2011) has a smaller impact than the reconstruction by KK11 (Kaplan et al., 2011, 2012): averaged over our Roman Empire study domain (from $10°$ W to $50°$ E and from $20°$ N to $60°$ N), the annual mean land surface temperature increases by $0.10\,\mathrm{K}$ for the HYDE reconstruction (insignificant) and by $0.15\,\mathrm{K}$ for the reconstruction by KK11 (significant). The increases in KK11 are only significant in a rather small part of the considered region (parts of North Africa and the Middle East).

Contrary to the warming effects of land use, anthropogenic aerosol emissions induce a significant cooling in land surface temperature for all scenarios. The temperature decreases by $0.17\,\mathrm{K}$, $0.23\,\mathrm{K}$, and $0.46\,\mathrm{K}$ for the low, the intermediate, and the high emission scenarios, respectively. The cooling is due to aerosol-cloud interactions and takes place mainly over Central and Eastern Europe.

Looking at the combined effect on land surface temperature, the aerosol-induced cooling is generally stronger than the land-cover-induced warming when averaged over the study domain. However, the mean decrease in surface temperature is only significant for the high scenario ($-0.32\,\mathrm{K}$). When interpreting these changes in temperature, one should keep in mind that the ocean temperatures were prescribed and the changes are thus underestimated.

Around AD 100 temperatures in Europe (as well as China and the Northern Hemisphere in general) were warmer than the average over the last two millenia (PAGES 2k Consortium, 2013; Ge et al., 2013; Christiansen and Ljungqvist, 2012), an era that has been called the "Roman Warm Period". While our results imply that anthropogenic land cover change may have regionally contributed to this warming, aerosol-cloud interactions would have attenuated it, suggesting other causes of the Roman Warm Period, e.g. ocean dynamics or solar forcing.

Our simulations suggest that the impact of anthropogenic aerosol emissions could have been at least as important as the impact of anthropogenic land cover change on climate in AD 100. However, the impact of anthropogenic aerosol emissions crucially depends on the seasonality of natural aerosol emissions over land (e.g. fire emissions and biogenic emissions). If the model severely underestimated the natural CCN in winter and spring, then the impact of the anthropogenic aerosol emissions would be much smaller. Furthermore, the output of global aerosol-climate models often shows a large spread, and our model is most likely oversensitive to the changes in anthropogenic aerosol emissions due to the lowered minimum CDNC.

Our scenarios show that pasture burning could have been an important source of aerosol particles. A better understanding of the processes that drive the frequency, the seasonality, and the emissions of pasture burning could therefore be essential

to quantify the anthropogenic impact far back in time. These processes could be implemented in a vegetation-fire model that is coupled with an aerosol model. Further work should include collaboration with archaeologists and historians in order to incorporate better understanding of human behaviour in Classical Antiquity, particularly on fuel consumption and the timing and extent of the use of fire.

Competing interests. The authors declare that no competing interests are present.

Acknowledgements. This work was supported by a grant from the Swiss National Science Foundation (SNF) for the Sinergia project "Paleo fires from high-alpine ice cores" (CRSII2_154450) and by a grant from the Swiss National Supercomputing Centre (CSCS) under project ID

s652. We are deeply grateful to Thomas Raddatz, who provided temporally high resolution data of MPI-ESM to drive CBALONE-SPITFIRE. He also helped the main author with questions about JSBACH and its anthropogenic land cover scheme. We thank Robyn Veal, Edouard Davin, Luisa Ickes, Silvia Kloster, Tanja Stanelle, and David Neubauer for valuable inputs and discussions. Furthermore, we thank Jürgen Bader for providing SST and SIC of at that time unpublished MPI-ESM simulations and Silvia Kloster and Christian Reick for enabling collaborations between people from the MPI Hamburg and ETH Zürich. We generally thank the developers of the ECHAM-HAMMOZ model, which is developed by a consortium composed of ETH Zürich, Max Planck Institut für Meteorologie, Forschungszentrum Jülich, University of Oxford, the Finnish Meteorological Institute, and the Leibniz Institute for Tropospheric Research and is managed by the Center for Climate Systems Modeling (C2SM) at ETH Zürich. We also acknowledge all the people that made their published data available, e.g. the developers of CESM2.0 WACCM and the people contributing to CMIP6 input data and to the HYDE database.

Clim. Past Discuss., https://doi.org/10.5194/cp-2019-56
Manuscript under review for journal Clim. Past
Discussion started: 24 May 2019

References

Aalde, H., Gonzalez, P., Gytarsky, M., Krug, T., Kurz W, A., Lasco R, D., Martino D, L., McConkey B, G., Ogle S, M., Paustian, K., Raison, J., Ravindranath N, H., Schoene, D., Smith, P., Somogyi, Z., van, A. A., and Verchot, L.: Generic methodologies applicable to multiple land-use categories, chap. 2, 2006.

Albrecht, B.: Aerosols, Cloud Microphysics, and Fractional Cloudiness, Science, 245, 1227–1230, https://doi.org/10.1126/science.245.4923.1227, 1989.

Andres, R. J. and Kasgnoc, A. D.: A time-averaged inventory of subaerial volcanic sulfur emissions, Journal of Geophysical Research: Atmospheres, 103, 25 251–25 261, https://doi.org/10.1029/98JD02091, https://agupubs.onlinelibrary.wiley.com/doi/abs/10.1029/98JD02091, 1998.

Anklin, M. and Bales, R. C.: Recent increase in H2O2 concentration at Summit, Greenland, Journal of Geophysical Research: Atmospheres, 102, 19 099–19 104, https://doi.org/10.1029/97JD01485, 1997.

Ascoli, D. and Bovio, G.: Prescribed burning in Italy: issues, advances and challenges, iForest - Biogeosciences and Forestry, pp. 79–89, https://doi.org/10.3832/ifor0803-006, http://iforest.sisef.org/contents/?id=ifor0803-006, 2013.

Bader, J., Jungclaus, J., Krivova, N., Lorenz, S., Maycock, A., Raddatz, T., Schmidt, H., Toohey, M., Wu, C.-J., and Claussen, M.: Global temperature modes shed light on the Hologene temperature conundrum, Nat. Commun., 2019, in review.

Bathiany, S., Claussen, M., Brovkin, V., Raddatz, T., and Gayler, V.: Combined biogeophysical and biogeochemical effects of large-scale forest cover changes in the MPI earth system model, Biogeosciences, 7, 1383–1399, https://doi.org/10.5194/bg-7-1383-2010, https://www.biogeosciences.net/7/1383/2010/, 2010.

Bauer, S. E., Koch, D., Unger, N., Metzger, S. M., Shindell, D. T., and Streets, D. G.: Nitrate aerosols today and in 2030: a global simulation including aerosols and tropospheric ozone, Atmos. Chem. Phys., 7, 5043–5059, https://doi.org/10.5194/acp-7-5043-2007, https://www.atmos-chem-phys.net/7/5043/2007/, 2007.

Bender, F. A.-M., Frey, L., McCoy, D. T., Grosvenor, D. P., and Mohrmann, J. K.: Assessment of aerosol–cloud–radiation correlations in satellite observations, climate models and reanalysis, Climate Dyn., https://doi.org/10.1007/s00382-018-4384-z, https://doi.org/10.1007/s00382-018-4384-z, 2018.

Bergman, T., Kerminen, V.-M., Korhonen, H., Lehtinen, K. J., Makkonen, R., Arola, A., Mielonen, T., Romakkaniemi, S., Kulmala, M., and Kokkola, H.: Evaluation of the sectional aerosol microphysics module SALSA implementation in ECHAM5-HAM aerosol-climate model, Geosci. Model Dev., 5, 845–868, https://doi.org/10.5194/gmd-5-845-2012, 2012.

Bielenstein, H.: Wang Mang, the restoration of the Han dynasty, and Later Han, vol. 1 of *The Cambridge History of China*, p. 223–290, Cambridge University Press, https://doi.org/10.1017/CHOL9780521243278.005, 1986.

Bond, T. C., Streets, D. G., Yarber, K. F., Nelson, S. M., Woo, J.-H., and Klimont, Z.: A technology-based global inventory of black and organic carbon emissions from combustion, Journal of Geophysical Research: Atmospheres, 109, https://doi.org/10.1029/2003JD003697, https://agupubs.onlinelibrary.wiley.com/doi/abs/10.1029/2003JD003697, 2004.

Boucher, O., Randall, D., Artaxo, P., Bretherton, C., Feingold, G., Forster, P., Kerminen, V.-M., Kondo, Y., Liao, H., Lohmann, U., Rasch, P., Satheesh, S., Sherwood, S., Stevens, B., and Zhang, X.: Clouds and Aerosols. In: Climate Change 2013: The Physical Science Basis. Contribution of Working Group I to the Fifth Assessment Report of the Intergovernmental Panel on Climate Change [Stocker, T.F., D. Qin, G.-K. Plattner, M. Tignor, S.K. Allen, J. Boschung, A. Nauels, Y. Xia, V. Bex and P.M. Midgley (eds.)]., Cambridge University Press, Cambridge, United Kingdom and New York, NY, USA., 2013.

Boysen, L. R., Brovkin, V., Arora, V. K., Cadule, P., de Noblet-Ducoudré, N., Kato, E., Pongratz, J., and Gayler, V.: Global and regional effects of land-use change on climate in 21st century simulations with interactive carbon cycle, Earth Syst. Dyn., 5, 309–319, https://doi.org/10.5194/esd-5-309-2014, https://www.earth-syst-dynam.net/5/309/2014/, 2014.

Brännvall, M.-L., Bindler, R., Renberg, I., Emteryd, O., Bartnicki, J., and Billström, K.: The Medieval Metal Industry Was the Cradle of Modern Large-Scale Atmospheric Lead Pollution in Northern Europe, Environmental Science & Technology, 33, 4391–4395, https://doi.org/10.1021/es990279n, https://doi.org/10.1021/es990279n, 1999.

Brovkin, V., Raddatz, T., Reick, C. H., Claussen, M., and Gayler, V.: Global biogeophysical interactions between forest and climate, GEOPHYSICAL RESEARCH LETTERS, 36, https://doi.org/10.1029/2009GL037543, 2009.

Carslaw, K. S., Gordon, H., Hamilton, D. S., Johnson, J. S., Regayre, L. A., Yoshioka, M., and Pringle, K. J.: Aerosols in the Pre-industrial Atmosphere, Current Climate Change Reports, 3, 1–15, https://doi.org/10.1007/s40641-017-0061-2, https://doi.org/10.1007/s40641-017-0061-2, 2017.

Christiansen, B. and Ljungqvist, F. C.: The extra-tropical Northern Hemisphere temperature in the last two millennia: reconstructions of low-frequency variability, Clim. Past, 8, 765–786, https://doi.org/10.5194/cp-8-765-2012, https://www.clim-past.net/8/765/2012/, 2012.

Claussen, M., Brovkin, V., and Ganopolski, A.: Biogeophysical versus biogeochemical feedbacks of large-scale land cover change, Geophys. Res. Lett., 28, 1011–1014, https://doi.org/10.1029/2000GL012471, https://agupubs.onlinelibrary.wiley.com/doi/abs/10.1029/2000GL012471, 2001.

Crutzen, P. J. and Brühl, C.: A model study of atmospheric temperatures and the concentrations of ozone, hydroxyl, and some other photochemically active gases during the glcial, the pre-industrial Holocene and the present, Geophys. Res. Lett., 20, 1047–1050, 1993.

Donahue, N. M., Robinson, A. L., Stanier, C. O., and Pandis, S. N.: Coupled Partitioning, Dilution, and Chemical Aging of Semivolatile Organics, Environmental Science & Technology, 40, 2635–2643, https://doi.org/10.1021/es052297c, 2006.

Forster, P., Ramaswamy, V., Artaxo, P., Berntsen, T., Betts, R., Fahey, D., Haywood, J., Lean, J., Lowe, D., Myhre, G., Nganga, J., Prinn, R., Raga, G., Schulz, M., and Dorland, R. V.: 2007: Changes in Atmospheric Constituents and in Radiative Forcing., Cambridge University Press, Cambridge, United Kingdom and New York, NY, USA, 2007.

Ge, Q., Hao, Z., Zheng, J., and Shao, X.: Temperature changes over the past 2000 yr in China and comparison with the Northern Hemisphere, Clim. Past, 9, 1153–1160, https://doi.org/doi:10.5194/cp-9-1153-2013, 2013.

Goodchild, H.: Modelling Roman agricultural production in the middle Tiber Valley, Central Italy, Ph.D. thesis, 2007.

Gordon, H., Sengupta, K., Rap, A., Duplissy, J., Frege, C., Williamson, C., Heinritzi, M., Simon, M., Yan, C., Almeida, J., Tröstl, J., Nieminen, T., Ortega, I. K., Wagner, R., Dunne, E. M., Adamov, A., Amorim, A., Bernhammer, A.-K., Bianchi, F., Breitenlechner, M., Brilke, S., Chen, X., Craven, J. S., Dias, A., Ehrhart, S., Fischer, L., Flagan, R. C., Franchin, A., Fuchs, C., Guida, R., Hakala, J., Hoyle, C. R., Jokinen, T., Junninen, H., Kangasluoma, J., Kim, J., Kirkby, J., Krapf, M., Kürten, A., Laaksonen, A., Lehtipalo, K., Makhmutov, V., Mathot, S., Molteni, U., Monks, S. A., Onnela, A., Peräkylä, O., Piel, F., Petäjä, T., Praplan, A. P., Pringle, K. J., Richards, N. A. D., Rissanen, M. P., Rondo, L., Sarnela, N., Schobesberger, S., Scott, C. E., Seinfeld, J. H., Sharma, S., Sipilä, M., Steiner, G., Stozhkov, Y., Stratmann, F., Tomé, A., Virtanen, A., Vogel, A. L., Wagner, A. C., Wagner, P. E., Weingartner, E., Wimmer, D., Winkler, P. M., Ye, P., Zhang, X., Hansel, A., Dommen, J., Donahue, N. M., Worsnop, D. R., Baltensperger, U., Kulmala, M., Curtius, J., and Carslaw, K. S.: Reduced anthropogenic aerosol radiative forcing caused by biogenic new particle formation, Proceedings of the National Academy of Sciences, 113, 12 053–12 058, https://doi.org/10.1073/pnas.1602360113, http://www.pnas.org/content/113/43/12053, 2016.

Halmer, M. M., Schmicke, H.-U., and Graf, H.-F.: The annual volcanic gas input into the atmosphere, in particular into the stratosphere: a global data set for the past 100 years, J. Volcanol. Geotherm. Res., 115, 511–528, 2002.

Harris, W.: Defining and Detecting Mediterranean Deforestation, 800BCE to 700CE, pp. 173 – 194, Brill, Leiden, The Netherlands, https://brill.com/view/book/edcoll/9789004254053/B9789004254053_008.xml, 2013.

Hauglustaine, D. A., Balkanski, Y., and Schulz, M.: A global model simulation of present and future nitrate aerosols and their direct radiative forcing of climate, Atmos. Chem. Phys., 14, 11 031–11 063, https://doi.org/10.5194/acp-14-11031-2014, https://www.atmos-chem-phys.net/14/11031/2014/, 2014.

Hay, R. K. M.: Harvest index: a review of its use in plant breeding and crop physiology, Ann. Appl. Biol., 126, 197–216, 1995.

Henrot, A.-J., Stanelle, T., Schröder, S., Siegenthaler, C., Taraborrelli, D., and Schultz, M. G.: Implementation of the MEGAN (v2.1) biogenic emission model in the ECHAM6-HAMMOZ chemistry climate model, Geosci. Model Dev., 10, 903–926, https://doi.org/10.5194/gmd-10-903-2017, https://www.geosci-model-dev.net/10/903/2017/, 2017.

Hin, S.: The demography of Roman Italy, Cambridge University Press, 2013.

Hong, S., Candelone, J.-P., Patterson, C. C., and Boutron, C. F.: History of Ancient Copper Smelting Pollution During Roman and Medieval Times Recorded in Greenland Ice, Science, 272, 246–249, https://doi.org/10.1126/science.272.5259.246, http://science.sciencemag.org/content/272/5259/246, 1996.

Hoose, C., Kristjánsson, J. E., Iversen, T., Kirkevåg, A., Seland, O., and Gettelman, A.: Constraining cloud droplet number concentration in GCMs suppresses the aerosol indirect effect, Geophys. Res. Lett., 36, https://doi.org/10.1029/2009gl038568, https://doi.org/10.1029/2009GL038568, 2009.

Hopkins, K.: Taxes and Trade in the Roman Empire (200 B.C.–A.D. 400), Journal of Roman Studies, 70, 101–125, https://doi.org/10.2307/299558, 1980.

Hopkins, K.: Models, Ships and Staples, p. 213–268, Cambridge Classical Studies, Cambridge University Press, https://doi.org/10.1017/CBO9781139093552.009, 2017.

Janssen, E., Poblome, J., Claeys, J., Kint, V., Degryse, P., Marinova, E., and Muys, B.: Fuel for debating ancient economies. Calculating wood consumption at urban scale in Roman Imperial times, J. Archaeolog. Sci.: Rep., 11, 592 – 599, https://doi.org/https://doi.org/10.1016/j.jasrep.2016.12.029, http://www.sciencedirect.com/science/article/pii/S2352409X16303777, 2017.

Kaplan, J. O., Krumhardt, K. M., and Zimmermann, N.: The prehistoric and preindustrial deforestation of Europe, Quat. Sci. Rev., 28, 3016 – 3034, https://doi.org/https://doi.org/10.1016/j.quascirev.2009.09.028, http://www.sciencedirect.com/science/article/pii/S027737910900331X, 2009.

Kaplan, J. O., Krumhardt, K. M., Ellis, E. C., Ruddiman, W. F., Lemmen, C., and Goldewijk, K. K.: Holocene carbon emissions as a result of anthropogenic land cover change, The Holocene, 21, 775–791, https://doi.org/10.1177/0959683610386983, https://doi.org/10.1177/0959683610386983, 2011.

Kaplan, J. O., Krumhardt, K. M., and Zimmermann, N. E.: The effects of land use and climate change on the carbon cycle of Europe over the past 500 years, Global Change Biol., 18, 902–914, https://doi.org/10.1111/j.1365-2486.2011.02580.x, https://onlinelibrary.wiley.com/doi/abs/10.1111/j.1365-2486.2011.02580.x, 2012.

Kaplan, J. O., Pfeiffer, M., Kolen, J. C. A., and Davis, B. A. S.: Large Scale Anthropogenic Reduction of Forest Cover in Last Glacial Maximum Europe, PLoS One, 11, e0166 726, 2016.

Kessler, D. and Temin, P.: The organization of the grain trade in the early Roman Empire, The Economic History Review, 60, 313–332, https://doi.org/10.1111/j.1468-0289.2006.00360.x, https://onlinelibrary.wiley.com/doi/abs/10.1111/j.1468-0289.2006.00360.x, 2007.

Khan, M., Cooke, M., Utembe, S., Archibald, A., Derwent, R., Xiao, P., Percival, C., Jenkin, M., Morris, W., and Shallcross, D.: Global modeling of the nitrate radical (NO3) for present and pre-industrial scenarios, Atmos. Res., 164, 347 – 357, https://doi.org/http://dx.doi.org/10.1016/j.atmosres.2015.06.006, http://www.sciencedirect.com/science/article/pii/S0169809515001817, 2015.

Klein Goldewijk, K., Beusen, A., van Drecht, G., and de Vos, M.: The HYDE 3.1 spatially explicit database of human-induced global land-use change over the past 12,000 years, Global Ecol. Biogeogr., 20, 73–86, https://doi.org/10.1111/j.1466-8238.2010.00587.x, 2011.

Klein Goldewijk, K., Beusen, A., Doelman, J., and Stehfest, E.: Anthropogenic land use estimates for the Holocene – HYDE 3.2, Earth Syst. Sci. Data, 9, 927–953, https://doi.org/10.5194/essd-9-927-2017, https://www.earth-syst-sci-data.net/9/927/2017/, 2017.

Koch, D. and Del Genio, A. D.: Black carbon semi-direct effects on cloud cover: review and synthesis, Atmos. Chem. Phys., 10, 7685–7696, https://doi.org/10.5194/acp-10-7685-2010, https://www.atmos-chem-phys.net/10/7685/2010/, 2010.

Kokkola, H., Korhonen, H., Lehtinen, K. E. J., Makkonen, R., Asmi, A., Järvenoja, S., Anttila, T., Partanen, A.-I., Kulmala, M., Järvinen, H., Laaksonen, A., and Kerminen, V.-M.: SALSA – a Sectional Aerosol module for Large Scale Applications, Atmos. Chem. Phys., 8, 2469–2483, https://doi.org/10.5194/acp-8-2469-2008, 2008.

Kokkola, H., Kühn, T., Laakso, A., Bergman, T., Lehtinen, K. E. J., Mielonen, T., Arola, A., Stadtler, S., Korhonen, H., Ferrachat, S., Lohmann, U., Neubauer, D., Tegen, I., Drian, C. S.-L., Schultz, M. G., Bey, I., Stier, P., Daskalakis, N., Heald, C. L., and Romakkaniemi, S.: SALSA2.0: The sectional aerosol module of the aerosol–chemistry–climate model ECHAM6.3.0-HAM2.3-MOZ1.0, Geosci. Model Dev., 11, 3833–3863, 2018.

Kühn, T., Merikanto, J., Mielonen, T., Stadtler, S., Schultz, M., Hienola, A., Korhonen, H., Ferrachat, S., Lohmann, U., Neubauer, D., Tegen, I., Drian, C. S.-L., Rast, S., Schmidt, H., Stier, P., Lehtinen, K., and Kokkola, H.: SALSA2.0 – part 2: Implementation of a volatility basis set to model formation of secondary organic aerosol, Geosci. Model Dev., 2019, in preparation.

Lasslop, G., Thonicke, K., and Kloster, S.: SPITFIRE within the MPI Earth system model: Model development and evaluation, J. Adv. Model. Earth Syst., 6, 740–755, https://doi.org/10.1002/2013MS000284, 2014.

Lee, X., Goulden, M. L., Hollinger, D. Y., Barr, A., Black, T. A., Bohrer, G., Bracho, R., Drake, B., Goldstein, A., Gu, L., Katul, G., Kolb, T., Law, B. E., Margolis, H., Meyers, T., Monson, R., Munger, W., Oren, R., Paw U, K. T., Richardson, A. D., Schmid, H. P., Staebler, R., Wofsy, S., and Zhao, L.: Observed increase in local cooling effect of deforestation at higher latitudes, Nature, 479, 384, https://doi.org/10.1038/nature10588, 2011.

Lejeune, Q., Seneviratne, S. I., and Davin, E. L.: Historical land-cover change impacts on climate: comparative assessment of LUCID and CMIP5 multimodel experiments, AMS, 30, 1439–1459, https://doi.org/10.1175/JCLI-D-16-0213.s1., 2017.

Lelieveld, J., Peters, W., Dentener, F. J., and Krol, M. C.: Stability of tropospheric hydroxyl chemistry, Journal of Geophysical Research: Atmospheres, 107, ACH 17–1–ACH 17–11, https://doi.org/10.1029/2002JD002272, 2002.

Li, J., Li, Y., Bo, Y., and Xie, S.: High-resolution historical emission inventories of crop residue burning in fields in China for the period 1990–2013, Atmos. Environ., 138, 152 – 161, https://doi.org/https://doi.org/10.1016/j.atmosenv.2016.05.002, http://www.sciencedirect.com/science/article/pii/S135223101630334X, 2016a.

Li, Y., Zhao, M., Motesharrei, S., Mu, Q., Kalnay, E., and Li, S.: Local cooling and warming effects of forests based on satellite observations, Nat. Commun., 6, https://doi.org/10.1038/ncomms7603, 2015.

Li, Y., Henze, D. K., Jack, D., and Kinney, P. L.: The influence of air quality model resolution on health impact assessment for fine particulate matter and its components, Air Quality, Atmosphere & Health, 9, 51–68, https://doi.org/10.1007/s11869-015-0321-z, https://doi.org/10.1007/s11869-015-0321-z, 2016b.

Li, Y., Zhao, M., Mildrexler, D. J., Motesharrei, S., Mu, Q., Kalnay, E., Zhao, F., Li, S., and Wang, K.: Potential and Actual impacts of deforestation and afforestation on land surface temperature, J. Geophy. Res. Atmos., 121, 14 372–14 386, https://doi.org/10.1002/2016JD024969., 2016c.

Makra, L.: Anthropogenic Air Pollution in Ancient Times, History of Toxicology and Environmental Health, 2, 21–41, 2015.

Malanima, P.: Energy crisis and growth 1650–1850: the European deviation in a comparative perspective, Journal of Global History, 1, 101–121, https://doi.org/10.1017/S1740022806000064, 2006.

Malanima, P.: Energy Consumption in the Roman World, pp. 13 – 36, Brill, Leiden, The Netherlands, https://brill.com/view/book/edcoll/9789004254053/B9789004254053_003.xml, 2013.

Malm, W. C., Schichtel, B. A., Pitchford, M. L., Ashbaugh, L. L., and Eldred, R. A.: Spatial and monthly trends in speciated fine particle concentration in the United States, Journal of Geophysical Research: Atmospheres, 109, https://doi.org/10.1029/2003JD003739, https://agupubs.onlinelibrary.wiley.com/doi/abs/10.1029/2003JD003739, 2004.

Meinshausen, M., Vogel, E., Nauels, A., Lorbacher, K., Meinshausen, N., Etheridge, D. M., Fraser, P. J., Montzka, S. A., Rayner, P. J., Trudinger, C. M., Krummel, P. B., Beyerle, U., Canadell, J. G., Daniel, J. S., Enting, I. G., Law, R. M., Lunder, C. R., O'Doherty, S., Prinn, R. G., Reimann, S., Rubino, M., Velders, G. J. M., Vollmer, M. K., Wang, R. H. J., and Weiss, R.: Historical greenhouse gas concentrations for climate modelling (CMIP6), Geosci. Model Dev., 10, 2057–2116, https://doi.org/10.5194/gmd-10-2057-2017, https://www.geosci-model-dev.net/10/2057/2017/, 2017.

Mietz, M.: The fuel economy of public bathhouses in the Roman Empire, Master's thesis, Ghent University, Faculty of Arts and Philosophy, Campus Boekentoren, Blandijnberg 2, B-9000 Ghent, Belgium, 2016.

Montiel, C. and Kraus, D.: Best Practices of Fire Use - Prescribed Burning and Suppression Fire Programmes in Selected Case-Study Regions of Europe, 2010.

Morales-Molino, C., Vescovi, E., Krebs, P., Carlevaro, E., Kaltenrieder, P., Conedera, M., Tinner, W., and Colombaroli, D.: The role of human-induced fire and sweet chestnut (Castanea sativa Mill.) cultivation on the long-term landscape dynamics of the southern Swiss Alps, The Holocene, 25, 482–494, https://doi.org/10.1177/0959683614561884, https://doi.org/10.1177/0959683614561884, 2015.

Murray, L. T., Mickley, L. J., Kaplan, J. O., Sofen, E. D., Pfeiffer, M., and Alexander, B.: Factors controlling variability in the oxidative capacity of the troposphere since the Last Glacial Maximum, Atmos. Chem. Phys., 14, 3589–3622, https://doi.org/10.5194/acp-14-3589-2014, https://www.atmos-chem-phys.net/14/3589/2014/, 2014.

Naveh, Z.: The evolutionary significance of fire in the mediterranean region, Vegetatio, 29, 199–208, 1975.

PAGES 2k Consortium: Continental-scale temperature variability during the past two millennia, Nat. Geosci., 6, 339–346, https://doi.org/10.1038/ngeo1797, 2013.

Pfeiffer, M., Spessa, A., and Kaplan, J. O.: A model for global biomass burning in preindustrial time: LPJ-LMfire (v1.0), Geosci. Model Dev., 6, 643–685, https://doi.org/10.5194/gmd-6-643-2013, https://www.geosci-model-dev.net/6/643/2013/, 2013.

Pham, M., Müller, J.-F., Brasseur, G. P., Granier, C., and Mégie, G.: A three-dimensional study of the tropospheric sulfur cycle, J. Geophys. Res., 100, 26 061–26 092, 1995.

Pinto, J. P. and Khalil, M. A. K.: The stability of tropospheric OH during ice ages, inter-glacial epochs and modern times, Tellus, 43B, 347–352, 1991.

Rabin, S. S., Melton, J. R., Lasslop, G., Bachelet, D., Forrest, M., Hantson, S., Kaplan, J. O., Li, F., Mangeon, S., Ward, D. S., Yue, C., Arora, V. K., Hickler, T., Kloster, S., Knorr, W., Nieradzik, L., Spessa, A., Folberth, G. A., Sheehan, T., Voulgarakis, A., Kelley, D. I., Prentice, I. C., Sitch, S., Harrison, S., and Arneth, A.: The Fire Modeling Intercomparison Project (FireMIP), phase 1: experimental and

analytical protocols with detailed model descriptions, Geosci. Model Dev., 10, 1175–1197, https://doi.org/10.5194/gmd-10-1175-2017, https://www.geosci-model-dev.net/10/1175/2017/, 2017.

Raddatz, T. J., Reick, C. H., Knorr, W., Kattge, J., Roeckner, E., Schnur, R., Schnitzler, K.-G., Wetzel, P., and Jungclaus, J.: Will the tropical land biosphere dominate the climate–carbon cycle feedback during the twenty-first century?, Climate Dyn., 29, 565–574, https://doi.org/10.1007/s00382-007-0247-8, https://doi.org/10.1007/s00382-007-0247-8, 2007.

Reick, C. H., Raddatz, T., Brovkin, V., and Gayler, V.: Representation of natural and anthropogenic land cover change in MPI-ESM, J. Adv. Model. Earth Syst., 5, 459–482, https://doi.org/10.1002/jame.20022, https://agupubs.onlinelibrary.wiley.com/doi/abs/10.1002/jame.20022, 2013.

Sapart, C. J., Monteil, G., Prokopiou, M., van de Wal, R. S. W., Kaplan, J. O., Sperlich, P., Krumhardt, K. M., van der Veen, C., Houweling, S., Krol, M. C., Blunier, T., Sowers, T., Martinerie, P., Witrant, E., Dahl-Jensen, D., and Röckmann, T.: Natural and anthropogenic variations in methane sources during the past two millennia, Nature, 490, 85, http://dx.doi.org/10.1038/nature11461, 2012.

Schaap, M., van Loon, M., ten Brink, H. M., Dentener, F. J., and Builtjes, P. J. H.: Secondary inorganic aerosol simulations for Europe with special attention to nitrate, Atmos. Chem. Phys., 4, 857–874, 2004.

Scheidel, W.: Roman Population Size: The Logic of the Debate, Brill, 2008.

Scheidel, W.: Population and Demography, chap. 13, pp. 134–145, John Wiley & Sons, Ltd, https://doi.org/10.1002/9781444308372.ch13, https://onlinelibrary.wiley.com/doi/abs/10.1002/9781444308372.ch13, 2009.

Sigg, A. and Neftel, A.: Evidence for a 50% increase in H2O2 over the past 200 years from a Greenland ice core, Nature, 351, 557–559, 1991.

Sinclair, T. R.: Historical Changes in Harvest Index and Crop Nitrogen Accumulation, Crop Sci., 38, 1998.

Smit, H., Metzger, M., and Ewert, F.: Spatial distribution of grassland productivity and land use in Europe, Agric. Syst., 98, 208 – 219, https://doi.org/https://doi.org/10.1016/j.agsy.2008.07.004, http://www.sciencedirect.com/science/article/pii/S0308521X08000784, 2008.

Smith, A.: Provenance of Coals from Roman Sites in England and Wales, Britannia, 28, 297–324, https://doi.org/10.2307/526770, 1997.

Smith, M. C., Singarayer, J. S., Valdes, P. J., Kaplan, J. O., and Branch, N. P.: The biogeophysical climatic impacts of anthropogenic land use change during the Holocene, Clim. Past, 12, 923–941, https://doi.org/10.5194/cp-12-923-2016, https://www.clim-past.net/12/923/2016/, 2016.

Spurr, M. S.: Arable cultivation in Roman Italy, The Society for the Promotion of Roman Studies, 1986.

Stier, P., Feichter, J., Kinne, S., Kloster, S., Vignati, E., Wilson, J., Ganzeveld, L., Tegen, I., Werner, M., Balkanski, Y., Schulz, M., Boucher, O., Minikin, A., and Petzold, A.: The aerosol-climate model ECHAM5-HAM, Atmos. Chem. Phys., 5, 1125–1156, https://doi.org/10.5194/acp-5-1125-2005, http://www.atmos-chem-phys.net/5/1125/2005/, 2005.

Strandberg, G. and Kjellström, E.: Climate Impacts from Afforestation and Deforestation in Europe, Earth Interact, 23, 1–27, https://doi.org/10.1175/EI-D-17-0033.1, https://doi.org/10.1175/EI-D-17-0033.1, 2019.

Tegen, I., Neubauer, D., Ferrachat, S., Siegenthaler-Le Drian, C., Bey, I., Schutgens, N., Stier, P., Watson-Parris, D., Stanelle, T., Schmidt, H., Rast, S., Kokkola, H., Schultz, M., Schroeder, S., Daskalakis, N., Barthel, S., Heinold, B., and Lohmann, U.: The global aerosol–climate model ECHAM6.3–HAM2.3 – Part 1: Aerosol evaluation, Geosci. Model Dev., 12, 1643–1677, https://doi.org/10.5194/gmd-12-1643-2019, https://www.geosci-model-dev.net/12/1643/2019/, 2019.

Temin, P.: The Economy of the Early Roman Empire, J. Econ. Perspect., 20, 133–151, 2006.

Thonicke, K., Spessa, A., Prentice, I. C., Harrison, S. P., Dong, L., and Carmona-Moreno, C.: The influence of vegetation, fire spread and fire behaviour on biomass burning and trace gas emissions: results from a process-based model, Biogeosciences, 7, 1991–2011, https://doi.org/10.5194/bg-7-1991-2010, http://www.biogeosciences.net/7/1991/2010/, 2010.

Tinner, W., Conedera, M., Ammann, B., and Lotter, A. F.: Fire ecology north and south of the Alps since the last ice age, The Holocene, 15, 1214–1226, https://doi.org/10.1191/0959683605hl892rp, https://doi.org/10.1191/0959683605hl892rp, 2005.

Tinner, W., van Leeuwen, J. F., Colombaroli, D., Vescovi, E., van der Knaap, W., Henne, P. D., Pasta, S., D'Angelo, S., and Mantia, T. L.: Holocene environmental and climatic changes at Gorgo Basso, a coastal lake in southern Sicily, Italy, Quat. Sci. Rev., 28, 1498 – 1510, https://doi.org/10.1016/j.quascirev.2009.02.001, 2009.

Tsigaridis, K., Krol, M., Dentener, F. J., Balkanski, Y., Lathière, J., Metzger, S., Hauglustaine, D. A., and Kanakidou, M.: Change in global aerosol composition since preindustrial times, Atmos. Chem. Phys., 6, 5143–5162, https://doi.org/10.5194/acp-6-5143-2006, https://www.atmos-chem-phys.net/6/5143/2006/, 2006.

Turn, S. Q., Jenkins, B. M., Chow, J. C., Pritchett, L. C., Campbell, D., Cahill, T., and Whalen, S. A.: Elemental characterizationof particulate matter emitted from biomass burning: Wind tunnel derived source profiles for herbaceous and wood fuels, J. Geophys. Res., 102, 3683–3699, 1997.

Twomey, S.: Pollution and planetary albedo, Atmos. Environ., 8, 1251–1256, https://doi.org/10.1016/0004-6981(74)90004-3, 1974.

Twomey, S.: The Influence of Pollution on the Shortwave Albedo of Clouds, American Meteorological Society, 34, 1149–1152, https://doi.org/10.1175/1520-0469(1977)034<1149:TIOPOT>2.0.CO;2, 1977.

van Marle, M. J. E., Kloster, S., Magi, B. I., Marlon, J. R., Daniau, A.-L., Field, R. D., Arneth, A., Forrest, M., Hantson, S., Kehrwald, N. M., Knorr, W., Lasslop, G., Li, F., Mangeon, S., Yue, C., Kaiser, J. W., and van der Werf, G. R.: Historic global biomass burning emissions for CMIP6 (BB4CMIP) based on merging satellite observations with proxies and fire models (1750–2015), Geosci. Model Dev., 10, 3329–3357, https://doi.org/10.5194/gmd-10-3329-2017, https://www.geosci-model-dev.net/10/3329/2017/, 2017.

Veal, R.: Wood and Charcoal for Rome: Towards an Understanding of Ancient Regional Fuel Economics, pp. 388 – 406, Brill, Leiden, The Netherlands, https://brill.com/view/book/edcoll/9789004345027/B9789004345027_017.xml, 2017.

Veira, A., Kloster, S., Schutgens, N. A. J., and Kaiser, J. W.: Fire emission heights in the climate system – Part 2: Impact on transport, black carbon concentrations and radiation, Atmos. Chem. Phys., 15, 7173–7193, https://doi.org/10.5194/acp-15-7173-2015, 2015.

Warde, P.: Fear of Wood Shortage and the Reality of the Woodland in Europe, c.1450–1850, History Workshop Journal, 62, 28–57, https://doi.org/10.1093/hwj/dbl009, http://dx.doi.org/10.1093/hwj/dbl009, 2006.

Webb, J., Hutchings, N., Amon, B., Nielsen, O.-K., Phillips, R., and Dämmgen, U.: Field burning of agricultural residues, Tech. rep., EMEP/EEA emission inventory guidebook 2013, 2013.

White, K. D.: Fallowing, Crop Rotation, and Crop Yields in Roman Times, Agricultural History, 44, 281–290, http://www.jstor.org/stable/3741455, 1970.

Wilkenskjeld, S., Kloster, S., Pongratz, J., Raddatz, T., and Reick, C. H.: Comparing the influence of net and gross anthropogenic land-use and land-cover changes on the carbon cycle in the MPI-ESM, Biogeosciences, 11, 4817–4828, https://doi.org/10.5194/bg-11-4817-2014, https://www.biogeosciences.net/11/4817/2014/, 2014.

Wilks, D. S.: "The Stippling Shows Statistically Significant Grid Points": How Research Results are Routinely Overstated and Overinterpreted, and What to Do about It, B. Am. Meteorol. Soc., 97, 2263–2273, https://doi.org/10.1175/BAMS-D-15-00267.1, 2016.

Winckler, J., Reick, C. H., Luyssaert, S., Cescatti, A., Stoy, P. C., Lejeune, Q., Raddatz, T., Chlond, A., Heidkamp, M., and Pongratz, J.: Different response of surface temperature and air temperature to deforestation in climate models, Earth Syst. Dyn. Discuss., 2018, 1–17, https://doi.org/10.5194/esd-2018-66, https://www.earth-syst-dynam-discuss.net/esd-2018-66/, 2018.

Witcher, R.: Agricultural Production in Roman Italy, chap. 23, pp. 459–482, Wiley-Blackwell, https://doi.org/10.1002/9781118993125.ch23, https://onlinelibrary.wiley.com/doi/abs/10.1002/9781118993125.ch23, 2016.

Wood, T. S. and Baldwin, S.: Fuelwood and charcoal use in developing countries, Ann. Rev. Energy, 10, 407–429, 1985.

World Health Organisation: WHO Air quality guidelines for particulate matter, ozone, nitrogen dioxide and sulfur dioxid. Global update 2005. Summary of risk assessment., 2006.

Yevich, R. and Logan, J. A.: An assessment of biofuel use and burning of agricultural waste in the developing world, Global Biogeochem. Cycles, 17, https://doi.org/10.1029/2002GB001952, 2003.

Zhang, L., Liu, Y., and Hao, L.: contributions of open crop straw burning emissions to PM2.5 concentrations in China, Environ. Res. Lett., 11, 2016.